### Dear Reviewer,

We sincerely thank the reviewer for careful evaluation of our manuscript and for providing insightful and constructive comments. We appreciate the recognition of our work and the suggestions offered to improve its clarity and scientific rigor. In the responses below, the reviewer's original comments are reproduced in *italic* for clarity. Our point-by-point replies follow each comment and are marked in green. All corresponding changes have been made in the revised manuscript and are marked in blue. Line numbers refer to the revised manuscript unless otherwise noted.

#### **Comments from Reviewer I:**

This paper presents the ambient OOMs measurement in a complex urban environment in China. By combining binPMF with multiple sub-range spectral analysis, 2571 OOMs were successfully identified, 11 distinct factors were used to explain major OOM formation pathways: five daytime photochemical processes, four nighttime NO3-driven oxidation processes, and two regional mixed sources. This analysis achieved the first successful separation of sesquiterpene oxidation products in environmental measurements. In previous studies, these compounds were indistinguishable in traditional full-spectrum analyses due to their weak signals and overlapping temporal patterns with other nocturnal factors. In general, I think this paper is well-structured and easy to follow. However, I do have some concerns that need to be addressed before it can be accepted for publication.

## Major Comments:

#### 1. Clarifications on Factor Analysis in R1, R2, and R3

- In Figure 3, R1, R2, and R3 correspond to 6, 8, and 9 factors, respectively, whereas Figures S2-S4 in the SI indicates that 12 factors are required to explain the N2-MT-I factors in R1, and 11 factors are needed for both R2 and R3.
- (a) Figure S2 shows 5 NP-related factors, and Figure S3 shows 2 NP-related factors.
  Since the formation pathways of these ions were not discussed in the final analysis,
  would it be possible to re-perform the factor analysis after removing the NP-related ions?

## **Response:**

Thank you for the constructive suggestion. To evaluate the influence of NP-related ions on our factor analysis, we removed the major NP-related bins from the original mass spectra (e.g., the bins near 201 Th for C<sub>6</sub>H<sub>5</sub>NO<sub>3</sub>NO<sub>3</sub>) and re-performed the binPMF analysis. It is important to note that only bins associated with high-abundance NP signals were removed. Bins associated with lower-abundance NP species were retained, as they may be adjacent to non-NP OOMs with similar masses, and removing them could lose valuable information. The updated analysis yielded a new 8-factor

solution (Fig. R1), which we compared with the original solution through correlation analysis (Fig. R2).

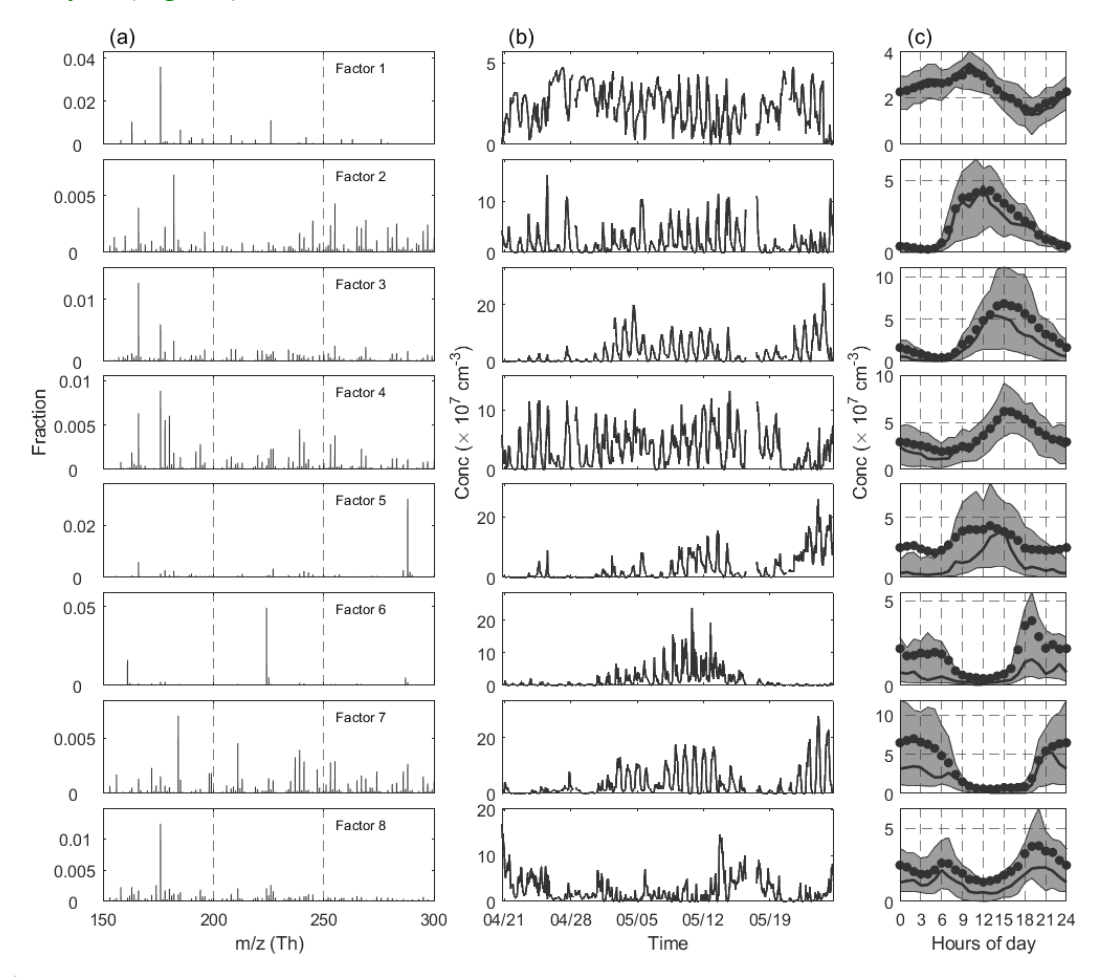


**Figure R1.** Selected binPMF solution for Range 1 after removing NP-related bins. (a) PMF factor profiles. (b) Time series of these factors. (c) Diurnal variations in PMF factors.

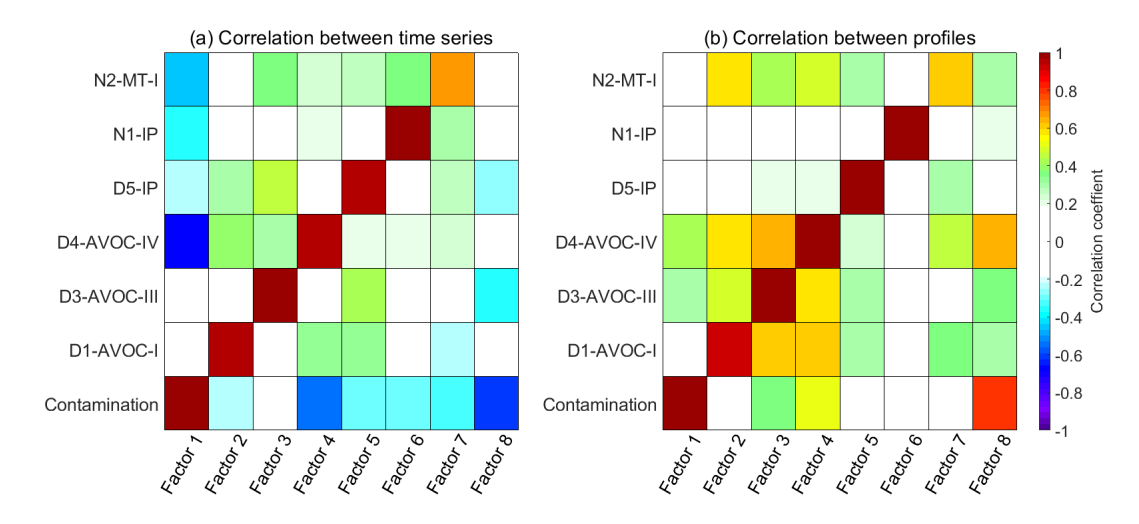


**Figure R2.** Comparison of the new 8-factor solution (after removal of NP-related bins) with the original solution. (a) Correlation of factor time series, and (b) correlation of factor profiles.

We found that all seven non-NP-related factors from the original solution were well reproduced. The additional factor (Factor 8) in the new solution consists primarily of perfluorinated acids and the residual NP-related ions. Unlike high-resolution PMF where individual ions can be excluded, our binPMF method operates directly on the raw spectral matrix. Therefore, to eliminate the influence of specific compounds, the corresponding mass spectral bins need to be removed. In this case, removing only the most prominent NP-related peaks resulted in the loss of nearly 2000 bins, which leads to a notable reduction in the spectral information available for analysis. Given this, we chose to retain the NP-related signals in our final analysis. In previous studies at our site (Liu et al., 2021, 2023), we also performed binPMF analysis and successfully separated NP-related factors. These studies consistently reveal their distinct chemical signatures compared to other OOMs. Because of these differences, NP-related components are usually resolved into individual factors with minimal overlap with other factors. Therefore, their exclusion in the current analysis is not expected to affect the overall factor resolution or interpretation. We have added this clarification to Line 247-261 in the revised manuscript for transparency.

#### Revised text:

Page 7, Line 247-261: In total, 17 merged factors are identified. These include five factors associated with daytime chemistry (denoted by the "D-" prefix), four factors linked to nighttime chemistry ("N-" prefix), two factors with no significant diurnal patterns and six factors excluded from the following discussion. Of these six disregarded factors, five factors are dominated by nitrophenol-related compounds, and one is characterized by fluorinated contaminants. The nitrophenol (NP) factors are not further analyzed in this study, as they have been extensively investigated in previous work (Cheng et al., 2021; Song et al., 2021; Chen et al., 2022). At this site, earlier binPMF analyses successfully separated NP factors (Liu et al., 2021, 2023), revealing their distinct chemical signatures compared to other OOMs. Due to these clear distinctions, NP-related components are typically resolved into separate factors with minimal overlap. Therefore, their exclusion in the current analysis is not expected to affect the overall factor resolution or interpretation. The contamination factor is primarily composed of various fluorinated compounds, mainly perfluorinated organic acids, which originated from the Teflon tubing used in our sampling system.

(b) Could you provide a detailed explanation of the contamination factors present in R1, R2, and R3?

## **Response:**

We appreciate the reviewer's question regarding the contamination factors observed in the three mass spectral subranges. In all three ranges (R1, R2, and R3), one factor is consistently dominated by fluorinated compounds, accounting for approximately 65% of the total signal intensity in that factor. These compounds are primarily identified as various types of fluorinated organic compounds, which were introduced from the sampling system, most likely through the Teflon tubing used in the instrument setup. The major compounds in this factor are shown in the Fig. R3. The main molecular structures feature perfluoroalkyl chains—in which all C-H bonds are replaced by C-F bonds—bearing one or two oxygen-containing functional groups (e.g., carboxyl, hydroxyl, or aldehyde). Representative examples include C<sub>x</sub>F<sub>2x+1</sub>COOH, C<sub>x</sub>F<sub>2x+1</sub>OH, and C<sub>x</sub>F<sub>2x</sub>CH<sub>2</sub>O<sub>2</sub>.

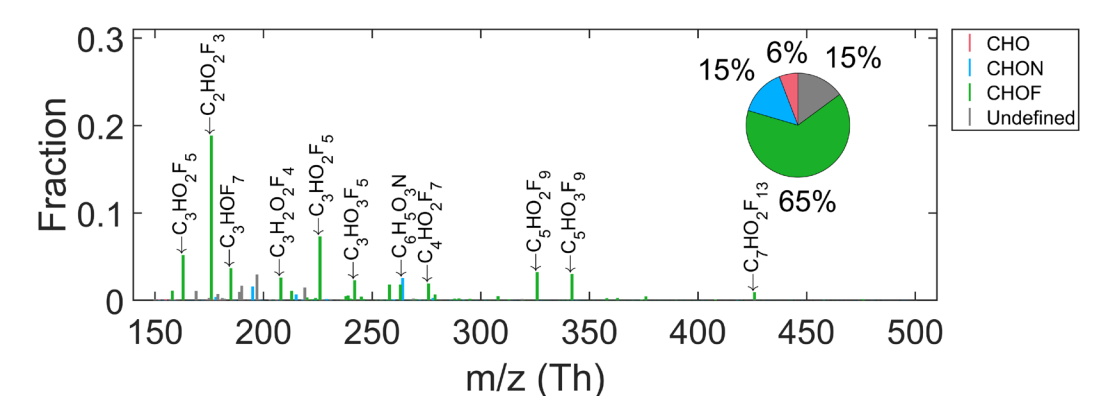


**Figure R3.** Mass spectra of the Contamination factor. The elemental formulas of major peaks are labeled above them. Peaks are colored by compound classes as indicated in the legend, and the fractions of peaks grouped by compound classes are reported in the pie chart.

(c) In R3, the factors D3-AVOC-III-1 and D3-AVOC-III-2 were merged before conducting correlation analysis with factors in the first two ranges. Could you elaborate on how this merging was specifically performed?

## **Response:**

The merging was performed as follows:

First, the time series of the two factors were summed to create the time series (ts) of the new merged factor. Then, the original time series and profiles of each factor were used to reconstruct their respective data matrices (A<sub>1</sub> and A<sub>2</sub>) by matrix multiplication. These two matrices were then added to obtain the data matrix A of the combined factor:

110 
$$A = A_1 + A_2 = (ts_1 \cdot pr_1) + (ts_2 \cdot pr_2)$$
 Eq. R1

Finally, the new profile (pr) of the merged factor was derived by solving the equation:

$$ts \cdot pr = A \qquad Eq. R2$$

- This approach preserved both the temporal and spectral information of the original
- two factors and ensured consistency in subsequent correlation analysis across subranges.
- We have included the above relevant descriptions in the supplement.

# 2. Interpreting OOM Factors Based on Precursor Compounds

- 117 CIMS data typically utilizes fingerprint molecules to characterize formation
- 118 pathways. However, in complex atmospheric environments, naming factors based on
- 119 their precursors (e.g., AVOC, isoprene, monoterpene) introduces significant
- interpretation challenges. For instance, regarding the D1-AVOC-I factor, the currently
- *presented evidence collectively supports its interpretation:*
- 122 It correlates relatively well with the 'Arom × OH' proxy.
- 123 This factor exhibits the highest average double bond equivalent (DBE).
- 124 The tracer molecules show comparability with existing laboratory studies.
- 125 For other factors, could additional discussion of results be incorporated in Sections
- 126 *3.2 and 3.3? Specific comments follow:*
- 127 (a) [D2-AVOC-II] Lines 291-292: "The first series represents typical aliphatic
- products, while the latter corresponds to second-generation aromatic products
- observed in laboratory studies." Please provide the reference/supporting evidence
- for this statement. Furthermore, it cannot be denied that  $C_xH_{2x-2}O_8N_2$  (e.g., C=10)
- may also originate from terpene oxidation (Luo et al., 2023).

## **Response:**

132

144

116

- We sincerely thank the reviewer for pointing out the limitations in our original
- statement. We agree that the previous wording regarding the interpretation of D2-
- AVOC-II was overly assertive and lacked sufficient supporting evidence. As suggested,
- we have revised the relevant description in the manuscript (Lines 336–342) to improve
- accuracy and clarity. Specifically, we have toned down the language and added
- supporting references from laboratory studies to substantiate the identification of
- second-generation aromatic products. In addition, we have incorporated the reviewer's
- important observation that compounds such as  $C_{10}H_{18}O_8N_2$  (i.e.,  $C_xH_{2x-2}O_8N_2$  with x =
- 141 10) could also originate from terpene oxidation, as demonstrated in Luo et al. (2023).
- 142 This possibility was indeed overlooked in the original manuscript, and we have now
- acknowledged it explicitly in the revised text:

## Revised text:

- 145 Page 11, Line 336-342: The first series also account for a substantial fraction in the
- Aliph-OOM factor in the summertime at this site (Liu et al., 2021). These near-saturated
- compounds are likely oxidation products of aliphatic precursors under strong NO<sub>x</sub>
- influence in urban air, as proposed in previous laboratory studies (Algrim and Ziemann,
- 2019; Wang et al., 2021). Notably, it cannot be denied that C<sub>10</sub>H<sub>18</sub>O<sub>8</sub>N<sub>2</sub> may also
- originate from terpene oxidation (Luo et al., 2023). The latter corresponds to second-

- generation aromatic products observed in laboratory studies (Tsiligiannis et al., 2019;
- 152 Wang et al., 2020).
- We appreciate this valuable suggestion, which has helped improve the robustness
- and balance of our factor interpretation.
- 155 (b) [D3-AVOC-III] Line 306: "These compounds are typical aromatic oxidation
- products." This conclusion appears overly assertive, as these products— $C_xH_{2x-4}O_5$
- 157 (7.3% abundance) and  $C_xH_{2x-2}O_5$  (6.0% abundance)—could also potentially
- originate from isoprene and monoterpene oxidation.

# **Response:**

159

160

was overly definitive. As noted, compounds such as C<sub>x</sub>H<sub>2x-4</sub>O<sub>5</sub> and C<sub>x</sub>H<sub>2x-2</sub>O<sub>5</sub> may also 161 originate from the oxidation of isoprene and monoterpenes. In fact, similar factors have 162 been reported in other ambient PMF studies. For example, Massoli et al. (2018) 163 identified an "isoprene afternoon" factor at a forested site, while Yan et al. (2016) 164 described a "Daytime type-3" factor, and Liu et al. (2021) observed a "Temp-related" 165 factor in an urban environment. These factors exhibited strong correlations with 166 temperature and were hypothesized to be associated with low-NO<sub>x</sub> daytime oxidation 167 of isoprene or fragment products from monoterpene oxidation. However, based on the 168 relatively high DBE values and the large contributions from C6-C8 compounds 169

We appreciate the reviewer's comment and fully agree that the original statement

- observed in this factor, we tend to attribute it predominantly to anthropogenic aromatic
- precursors. We have revised the manuscript accordingly (Lines 365–372) to reflect a
- more cautious interpretation and now present this factor as likely influenced by
- aromatic compounds but potentially containing contributions from biogenic sources as
- 174 well:

175

### Revised text:

- Page 12, Line 365-372: While their high DBE values and relatively high contributions from C6-C8 species suggest a strong influence from aromatic oxidation, we acknowledge that contributions from isoprene and monoterpene oxidation under low-NO<sub>x</sub> conditions cannot be ruled out. Similar factors were identified in previous studies, including an "isoprene afternoon" factor at a forest site in Alabama (Massoli et al., 2018), a "Daytime type-3" factor at a rural site in Finland (Yan et al., 2016), and a "Temp-related" factor in an urban environment (Liu et al., 2021), all showing
- temperature dependence and potential biogenic influence.
- Page 12, Line 382-384: Therefore, we propose this factor represents a characteristic photochemical process associated with O<sub>3</sub> formation, dominated by anthropogenic VOCs, but with possible contributions from biogenic sources as well.
- We thank the reviewer again for this important observation, which has led to a more
- nuanced and evidence-based discussion of this factor.

(c) [D4-AVOC-IV] The fingerprint molecules  $C_xH_{2x-2}O_4$  and  $C_xH_{2x-1,2x-3}O_6N$  are currently grouped within the same factor. However, are there laboratory studies showing shared precursors for these compounds or similar formation pathway?

## **Response:**

Thank you for this insightful comment. We agree that the co-occurrence of these molecular families requires careful interpretation. Although the formation mechanism of this factor is still under investigation, we propose that C<sub>x</sub>H<sub>2x-2,2x-4</sub>O<sub>4</sub> and C<sub>x</sub>H<sub>2x-1,2x-1</sub> 3O<sub>6</sub>N can be produced from a common RO<sub>2</sub> precursor (C<sub>x</sub>H<sub>2x-1</sub>O<sub>5</sub>) through different reaction branches with NO. Specifically, C<sub>x</sub>H<sub>2x-2</sub>O<sub>4</sub> compounds may form via the RO pathway, leading to carbonyl products, while C<sub>x</sub>H<sub>2x-1</sub>O<sub>6</sub>N compounds are typically formed via direct reaction of RO2 with NO to yield organic nitrates RONO2. Furthermore, a similar relationship is observed between C<sub>x</sub>H<sub>2x-3</sub>O<sub>6</sub>N and C<sub>x</sub>H<sub>2x-4</sub>O<sub>4</sub>, another group present in this factor (6.6%, Table S4), and C<sub>x</sub>H<sub>2x-2</sub>N<sub>2</sub>O<sub>8</sub> (4.8%, Table S4) found in the R2 range. These observations suggest that these species may indeed share precursors and form via alternative RO<sub>2</sub> termination channels influenced by NO levels. These two branches result in products differing by one HNO2 unit, suggesting a mechanistic link. A similar distribution of carbonyls and organic nitrates has been observed in laboratory experiments of alkane oxidation with added NO, supporting our interpretation (Wang et al., 2021). We have added this discussion in the revised manuscript (Lines 394-421) and clarified that, while the exact mechanisms remain uncertain, existing evidence supports the plausibility of a shared precursor-based formation for these compounds:

### Revised text:

Page 12, Line 394-421: While direct laboratory evidence linking these molecular series to a common formation pathway is limited, theoretical considerations and recent chamber studies support their possible co-generation. Both C<sub>x</sub>H<sub>2x-2</sub>O<sub>4</sub> and C<sub>x</sub>H<sub>2x-1</sub>O<sub>6</sub>N can be derived from the same RO<sub>2</sub> precursor (C<sub>x</sub>H<sub>2x-1</sub>O<sub>5</sub>) through different termination pathways with NO. The former may form via RO radical intermediates (C<sub>x</sub>H<sub>2x-1</sub>O<sub>4</sub>) that undergo further oxidation to produce carbonyl-containing compounds, whereas the latter results from direct NO addition to RO<sub>2</sub> forming RONO<sub>2</sub>. The mass difference between these products corresponds to a loss of one HNO<sub>2</sub> unit. A similar relationship applies between C<sub>x</sub>H<sub>2x-4</sub>O<sub>4</sub> (Table S4) and C<sub>x</sub>H<sub>2x-3</sub>O<sub>6</sub>N, as well as C<sub>x</sub>H<sub>2x-2</sub>N<sub>2</sub>O<sub>8</sub> in R2. Recent laboratory experiments investigating the OH oxidation of alkanes under varying NO levels also observed concurrent production of carbonyl species and organic nitrates, supporting this mechanistic linkage (Wang et al., 2021). These observations reinforce the idea that the co-occurrence of these compounds in the same factor likely reflects different chemical pathways stemming from shared precursors.

(d) Line351: What is the relative importance of ozonolysis for these nighttime factors?

## Response:

We thank the reviewer for this insightful comment regarding the potential role of ozonolysis in the formation of nighttime OOM factors. Our measurements at this site indicate that nighttime ozone concentrations often remain elevated, as shown in the Fig. S8a.

To better assess the relative importance of ozonolysis, we compared the nighttime (18:00–0:00 LT) reactivities (P = k[oxidant][VOC]) of O<sub>3</sub> and NO<sub>3</sub> toward selected BVOCs, including isoprene (IP) and α-pinene (MT). Here, k values were obtained from the Master Chemical Mechanism (MCM v3.3.1; http://mcm.york.ac.uk/, last access: 20 June 2025), and due to the lack of direct NO<sub>3</sub> measurements at this site, its concentration was simulated using the Framework for 0-D Atmospheric Modeling (F0AM) (Wolfe et al., 2016). The results are presented in Fig. S8b.

We found that for IP and MT, NO<sub>3</sub>-driven chemistry clearly dominates over ozonolysis, owing to much higher reaction rate constants of NO<sub>3</sub> (3–5 orders of magnitude greater than those of O<sub>3</sub>), even though O<sub>3</sub> concentrations are higher than those of NO<sub>3</sub> at night.

In addition, the molecular composition of these nighttime factors further supports the dominance of NO<sub>3</sub> chemistry. All four nighttime factors exhibit a high proportion of organic nitrate species (>80%), which are unlikely to originate from ozonolysis alone. O<sub>3</sub>-induced formation of organic nitrates typically requires the presence of NO, which remains at low levels during nighttime at our site.

Furthermore, each nighttime factor contains distinct RO<sub>2</sub> radicals that are characteristic of NO<sub>3</sub>-driven oxidation: C<sub>5</sub>H<sub>8</sub>O<sub>5</sub>N (from isoprene), C<sub>10</sub>H<sub>16</sub>O<sub>x</sub>N (from monoterpenes), and C<sub>15</sub>H<sub>24</sub>NO<sub>x</sub> (from sesquiterpenes). In contrast, we did not observe RO<sub>2</sub> species commonly associated with ozonolysis pathways, such as C<sub>10</sub>H<sub>15</sub>O<sub>x</sub> or C<sub>15</sub>H<sub>23</sub>O<sub>x</sub>, which have been reported in laboratory studies of O<sub>3</sub>–BVOC reactions (Kirkby et al., 2016; Richters et al., 2016; Dada et al., 2023).

These findings further support the conclusion that NO<sub>3</sub> oxidation plays the dominant role in driving nighttime OOM formation at our site. However, we cannot rule out a potential contribution from ozone oxidation, given the relatively high ozone concentrations observed during the night. We have incorporated this discussion into the revised manuscript, with additional supporting figure and references.

### Revised text:

*Page 13, Line 443-447:* However, considering that ozone concentrations remain relatively high during nighttime at this site (Fig. S8a), we cannot exclude a potential contribution from ozonolysis. The following four factors exhibit clear chemical signatures associated with biogenic volatile organic compounds (BVOCs) and their nighttime oxidation, with NO<sub>3</sub> chemistry playing a dominant role.

*Page 14, Line 515-518:* Nevertheless, given the high reactivity of sesquiterpenes toward ozone (Gao et al., 2022), and the elevated nighttime O<sub>3</sub> concentrations

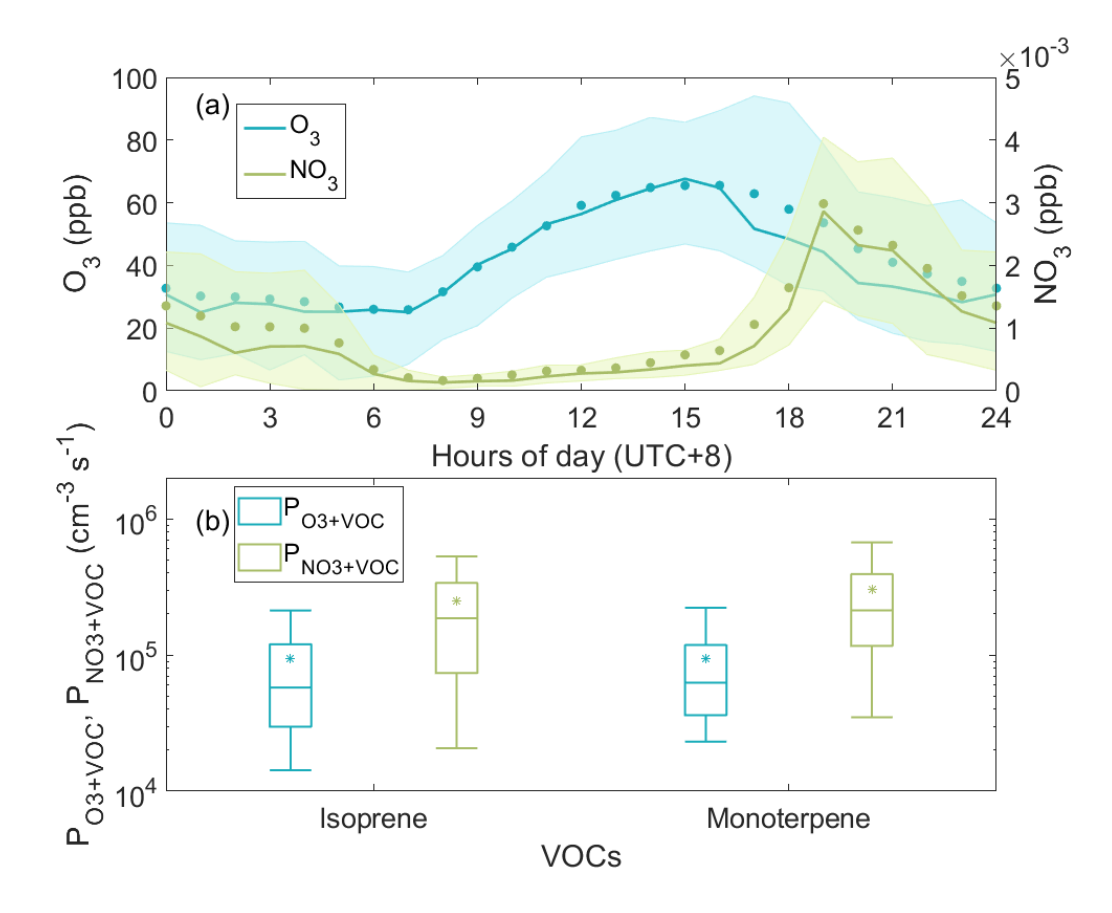


**Figure S8.** (a) Diurnal variations of O<sub>3</sub> and NO<sub>3</sub> radical. (b) Box plot of the oxidation reaction rates of isoprene and monoterpene by O<sub>3</sub> and NO<sub>3</sub> radical at nighttime.

(e) [N1-IP] Given that the RO<sub>2</sub> radical C<sub>5</sub>H<sub>8</sub>NO<sub>5</sub> accounts for 57.4% of the total factor intensity, while no higher-oxygen-number isoprene-RO<sub>2</sub> radicals were detected, here recommend to plot the time series of C<sub>5</sub>H<sub>8</sub>NO<sub>5</sub> and demonstrate its correlation with the factor.

## **Response:**

We appreciate the reviewer's suggestion. To address this, we have added a figure (Fig. S9) showing the time series of C<sub>5</sub>H<sub>8</sub>NO<sub>5</sub> (derived from direct peak fitting without binPMF) alongside the N1-IP factor concentration, as well as a scatter plot of their correlation. As shown, the time series of C<sub>5</sub>H<sub>8</sub>NO<sub>5</sub> closely follows the temporal trend of the N1-IP factor. The Pearson correlation coefficient reaches 0.98, confirming that C<sub>5</sub>H<sub>8</sub>NO<sub>5</sub> serves as a representative tracer for this factor.

## Revised text:

*Page 14, Line 458-460:* A peak-fitted time series of C<sub>5</sub>H<sub>8</sub>O<sub>5</sub>N was extracted and compared to the time series of the N1-IP factor. As shown in Fig. S9, the two are highly

correlated (R = 0.98), demonstrating that this compound can serve as a representative tracer for this factor.

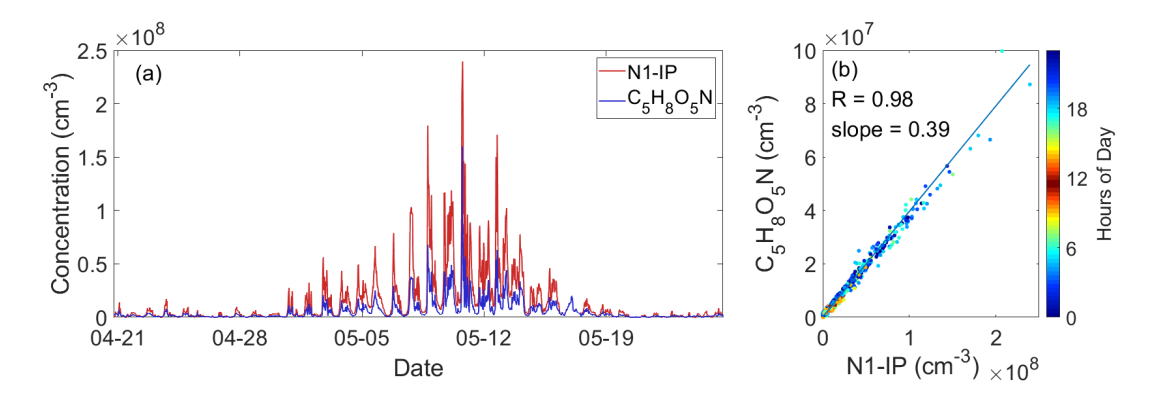


**Figure S9.** Time series and correlation analysis between the N1-IP factor and C<sub>5</sub>H<sub>8</sub>O<sub>5</sub>N. (a) Temporal evolution of the N1-IP factor (red) and C<sub>5</sub>H<sub>8</sub>O<sub>5</sub>N (blue) obtained from direct peak fitting. (b) Correlation between C<sub>5</sub>H<sub>8</sub>O<sub>5</sub>N and the N1-IP factor, colored by hours of day.

(f) [N3-MT-II] From the diurnal pattern, the formation of this factor can be affected by O3 oxidation.

## **Response:**

Thank you for the insightful comment. We agree that the formation of the N3-MT-II factor is likely influenced by multiple oxidants, and ozonolysis may indeed contribute to some extent.

As discussed in Section 2 (d), although O<sub>3</sub> is present at relatively high levels during nighttime at this site, the calculated reaction rate indicates that O<sub>3</sub> oxidation of monoterpenes is significantly slower than NO<sub>3</sub> oxidation.

Furthermore, 98% of the compounds in this factor are organic nitrates, and 84% of them contain two or more nitrogen atoms (Fig. 4). Given the low nighttime NO concentrations at our site, it is difficult for these compounds to be formed efficiently through successive ozonolysis and NO termination steps. Such a pathway is therefore unlikely to be a major contributor to this factor.

Finally, according to current mechanisms,  $O_3$  + monoterpene reactions followed by NO addition are expected to produce  $C_{10}H_{15}NO_x$  and  $C_{10}H_{14}N_2O_x$ , where the DBE remains unchanged from the precursor (DBE = 3). In contrast, the compounds in this factor are characterized by DBE < 3 (Table S9), which is inconsistent with typical  $O_3$  oxidation products. Taken together, we interpret the N3-MT-II factor as a product of multi-oxidant chemistry involving NO<sub>3</sub>, OH, and possibly O<sub>3</sub>, particularly at the daynight transitions. For example, nighttime NO<sub>3</sub>-initiated products may undergo further OH or O<sub>3</sub> oxidation after sunrise, or vice versa. The high abundance of multi-nitrates in this factor supports the idea of sequential oxidation steps under varying oxidant conditions. We have clarified this point in the revised manuscript to avoid any ambiguity.

#### Revised text:

Page 14, Line 493-503: This suggests that NO<sub>3</sub>-initiated oxidation of monoterpenes at night is followed by further oxidation in the morning, potentially involving OH and O<sub>3</sub>, leading to the observed multi-nitrate species. Furthermore, some of the nighttime concentrations may arise from daytime oxidation products that undergo additional NO<sub>3</sub>-driven oxidation during the night. Overall, this factor represents multi-generational oxidation products, involving various oxidants during the transition between day and night.

327

328

329

330

331

332

333

334

335

336

337

338

339

340

341

342

343

344

345346

347

348

349

350

351

319

320

321

322323

324

325

326

(g) [Mixed-MT] The current characterization of this factor appears incomplete and need additional explanation.

# **Response:**

We agree that the characterization of the Mixed-MT factor could benefit from further clarification. We have revised the manuscript to provide additional discussion on its chemical composition and potential formation pathways.

## Revised text:

Page 16, Line 551-567: This factor exhibits a complex molecular composition with a broad carbon number distribution (C<sub>5</sub>-C<sub>15</sub>), suggesting contributions from multiple precursor classes. While monoterpene-derived dinitrates (C<sub>10</sub>H<sub>16</sub>O<sub>8,9</sub>N<sub>2</sub>, C<sub>10</sub>H<sub>18</sub>O<sub>8</sub>N<sub>2</sub>) dominate the composition and indicate multi-generational oxidation, the presence of a wide range of oxidation products implies the involvement of both biogenic and anthropogenic sources. Notably, the most abundant compounds in R2 are C<sub>x</sub>H<sub>2x-3,2x-</sub> 5O<sub>6</sub>N, while in R3, the corresponding species are mainly C<sub>x</sub>H<sub>2x-2,2x-4</sub>O<sub>8</sub>N<sub>2</sub> (Table S11), differing by one HNO2 group. This pattern closely resembles that observed in the D4-AVOC-IV factor, further supporting the involvement of NO in the formation pathways. The high organic nitrate fraction (84%) further supports this interpretation. Taking the C<sub>10</sub> compounds as an illustrative example, species such as C<sub>10</sub>H<sub>17</sub>NO<sub>5-8</sub> are consistent with OH oxidation products of  $\alpha$ - and  $\beta$ -pinene observed in laboratory studies, while C<sub>10</sub>H<sub>18</sub>N<sub>2</sub>O<sub>8,9</sub> are likely formed through subsequent generation reactions. Additionally, the presence of C<sub>10</sub>H<sub>15</sub>NO<sub>5-7</sub> suggests a contribution from O<sub>3</sub>-initiated oxidation pathways. Altogether, these observations imply that this factor reflects a mixture of oxidation processes involving both OH and O<sub>3</sub>, rather than being dominated by a single oxidant or precursor type.

352

353

354

355

356

357

## 3. Mixed-Precursor Effects on Volatility Estimation

In the discussion of OOM volatility, the authors state: "The identification of monoterpene-related compounds was based on the approach proposed by Nie et al. (2022), where OOMs with DBE=2 that appeared in the PMF monoterpene-related factors were classified as monoterpene OOMs." This precursor-dependent

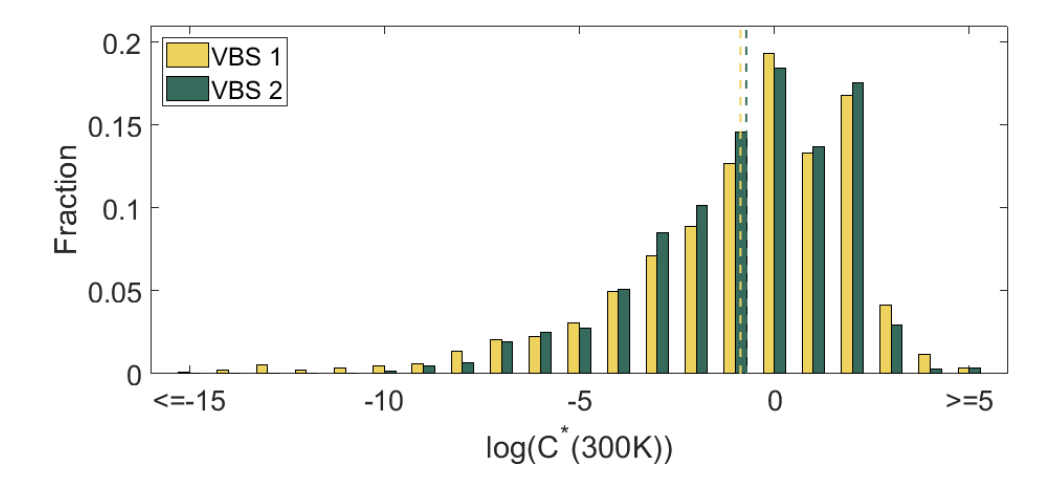
classification approach introduces additional uncertainty to the volatility distribution shown in Figure 5, particularly for factors like Mixed-MT where precursors are not exclusively monoterpenes.

## **Response:**

Thank you for pointing this out. We acknowledge that the original description of our classification method was unclear and contained a misstatement. In our analysis, we adopted a modified version of the classification proposed by Nie et al. (2022), in which terpene-related OOMs were identified within the terpene-dominated PMF factors (N2-MT-I, N3-MT-II, N4-SQT, and Mixed-MT). Specifically, we classified compounds as terpene OOMs with DBE between 2 and 4. For these terpene OOMs, we estimated their saturation vapor concentrations using the parameterization proposed by Mohr et al. (2019), which considers the influence of hydroperoxide on volatility.

We agree that this precursor-based classification remains a simplified approach and introduces some degree of uncertainty, particularly for mixed-source factors such as Mixed-MT. In urban environments, distinguishing terpene oxidation products from those originating from aromatic VOCs remains challenging, and the volatility estimates for such factors are subject to potential overlaps and misclassifications.

To further evaluate the effect of this classification on volatility distributions, we included an additional analysis (Fig. R4) comparing the resulting volatility distribution used in our study (VBS 1) with an alternative scheme (VBS 2) where all OOMs were treated using the Mohr method. The differences between the two schemes illustrate the uncertainty introduced by precursor-based volatility classification, but also fall within the expected range of variation caused by using different, yet reasonable, parameterizations. Although this factor is of mixed origin, we believe that monoterpenes still represent the dominant contributor, and therefore applying this volatility correction provides a more realistic representation than using a generic parameterization for all components.



- Figure R4. Comparison of volatility distributions (log C\* at 300 K) for the Mixed-MT
- factor using two different methods for estimating saturation concentration. The dashed
- 388 lines indicate the mean log C\* values for each method.
- 389 Minor Comment:
- 390 Line 192: C6H5OHNO3- is incorrect.
- 391 Line 306: should be Table S3.
- 392 **Response:**
- Thank you for pointing these out. We have corrected the molecular formula and
- updated the reference to Table S3 in the revised manuscript.

Reference:

395

396

- 397 Algrim, L. B. and Ziemann, P. J.: Effect of the Hydroxyl Group on Yields and
- 398 Composition of Organic Aerosol Formed from OH Radical-Initiated Reactions of
- 399 Alcohols in the Presence of NO  $_x$ , ACS Earth Space Chem., 3, 413–423,
- https://doi.org/10.1021/acsearthspacechem.9b00015, 2019.
- 401 Chen, Y., Zheng, P., Wang, Z., Pu, W., Tan, Y., Yu, C., Xia, M., Wang, W., Guo, J.,
- 402 Huang, D., Yan, C., Nie, W., Ling, Z., Chen, Q., Lee, S., and Wang, T.: Secondary
- 403 Formation and Impacts of Gaseous Nitro-Phenolic Compounds in the Continental
- 404 Outflow Observed at a Background Site in South China, Environ. Sci. Technol., 56,
- 405 6933–6943, https://doi.org/10.1021/acs.est.1c04596, 2022.
- Cheng, X., Chen, Q., Li, Y., Huang, G., Liu, Y., Lu, S., Zheng, Y., Qiu, W., Lu, K., Qiu,
- 407 X., Bianchi, F., Yan, C., Yuan, B., Shao, M., Wang, Z., Canagaratna, M. R., Zhu, T., Wu,
- 408 Y., and Zeng, L.: Secondary Production of Gaseous Nitrated Phenols in Polluted Urban
- 409 Environments, Environ. Sci. Technol., 55, 4410–4419,
- 410 https://doi.org/10.1021/acs.est.0c07988, 2021.
- Dada, L., Stolzenburg, D., Simon, M., Fischer, L., Heinritzi, M., Wang, M., Xiao, M.,
- Vogel, A. L., Ahonen, L., Amorim, A., Baalbaki, R., Baccarini, A., Baltensperger, U.,
- Bianchi, F., Daellenbach, K. R., DeVivo, J., Dias, A., Dommen, J., Duplissy, J.,
- Finkenzeller, H., Hansel, A., He, X.-C., Hofbauer, V., Hoyle, C. R., Kangasluoma, J.,
- Kim, C., Kürten, A., Kvashnin, A., Mauldin, R., Makhmutov, V., Marten, R., Mentler,
- B., Nie, W., Petäjä, T., Quéléver, L. L. J., Saathoff, H., Tauber, C., Tome, A., Molteni,
- 417 U., Volkamer, R., Wagner, R., Wagner, A. C., Wimmer, D., Winkler, P. M., Yan, C., Zha,
- Q., Rissanen, M., Gordon, H., Curtius, J., Worsnop, D. R., Lehtipalo, K., Donahue, N.
- M., Kirkby, J., El Haddad, I., and Kulmala, M.: Role of sesquiterpenes in biogenic new
- particle formation, Sci. Adv., 9, eadi5297, https://doi.org/10.1126/sciadv.adi5297, 2023.
- Gao, L., Song, J., Mohr, C., Huang, W., Vallon, M., Jiang, F., Leisner, T., and Saathoff,
- 422 H.: Kinetics, SOA yields, and chemical composition of secondary organic aerosol from

- $\beta$  -caryophyllene ozonolysis with and without nitrogen oxides between 213 and 313 K,
- 424 Atmos. Chem. Phys., 22, 6001–6020, https://doi.org/10.5194/acp-22-6001-2022, 2022.
- Kirkby, J., Duplissy, J., Sengupta, K., Frege, C., Gordon, H., Williamson, C., Heinritzi,
- 426 M., Simon, M., Yan, C., Almeida, J., Tröstl, J., Nieminen, T., Ortega, I. K., Wagner, R.,
- 427 Adamov, A., Amorim, A., Bernhammer, A.-K., Bianchi, F., Breitenlechner, M., Brilke,
- 428 S., Chen, X., Craven, J., Dias, A., Ehrhart, S., Flagan, R. C., Franchin, A., Fuchs, C.,
- Guida, R., Hakala, J., Hoyle, C. R., Jokinen, T., Junninen, H., Kangasluoma, J., Kim,
- J., Krapf, M., Kürten, A., Laaksonen, A., Lehtipalo, K., Makhmutov, V., Mathot, S.,
- Molteni, U., Onnela, A., Peräkylä, O., Piel, F., Petäjä, T., Praplan, A. P., Pringle, K.,
- Rap, A., Richards, N. A. D., Riipinen, I., Rissanen, M. P., Rondo, L., Sarnela, N.,
- 433 Schobesberger, S., Scott, C. E., Seinfeld, J. H., Sipilä, M., Steiner, G., Stozhkov, Y.,
- Stratmann, F., Tomé, A., Virtanen, A., Vogel, A. L., Wagner, A. C., Wagner, P. E.,
- Weingartner, E., Wimmer, D., Winkler, P. M., Ye, P., Zhang, X., Hansel, A., Dommen,
- J., Donahue, N. M., Worsnop, D. R., Baltensperger, U., Kulmala, M., Carslaw, K. S.,
- and Curtius, J.: Ion-induced nucleation of pure biogenic particles, Nature, 533, 521-
- 438 526, https://doi.org/10.1038/nature17953, 2016.
- 439 Liu, Y., Nie, W., Li, Y., Ge, D., Liu, C., Xu, Z., Chen, L., Wang, T., Wang, L., Sun, P.,
- 440 Qi, X., Wang, J., Xu, Z., Yuan, J., Yan, C., Zhang, Y., Huang, D., Wang, Z., Donahue,
- N. M., Worsnop, D., Chi, X., Ehn, M., and Ding, A.: Formation of condensable organic
- vapors from anthropogenic and biogenic volatile organic compounds (VOCs) is
- strongly perturbed by NOx in eastern China, Atmos. Chem. Phys., 21, 14789–14814,
- 444 https://doi.org/10.5194/acp-21-14789-2021, 2021.
- Liu, Y., Liu, C., Nie, W., Li, Y., Ge, D., Chen, L., Zhu, C., Wang, L., Zhang, Y., Liu, T.,
- 446 Qi, X., Wang, J., Huang, D., Wang, Z., Yan, C., Chi, X., and Ding, A.: Exploring
- condensable organic vapors and their co-occurrence with PM 2.5 and O 3 in winter in
- 448 Eastern China, Environ. Sci.: Atmos., 3, 282–297,
- 449 https://doi.org/10.1039/D2EA00143H, 2023.
- Luo, H., Vereecken, L., Shen, H., Kang, S., Pullinen, I., Hallquist, M., Fuchs, H.,
- Wahner, A., Kiendler-Scharr, A., Mentel, T. F., and Zhao, D.: Formation of highly
- 452 oxygenated organic molecules from the oxidation of limonene by OH radical:
- significant contribution of H-abstraction pathway, Atmos. Chem. Phys., 23, 7297–7319,
- 454 https://doi.org/10.5194/acp-23-7297-2023, 2023.
- 455 Massoli, P., Stark, H., Canagaratna, M. R., Krechmer, J. E., Xu, L., Ng, N. L., Mauldin,
- 456 R. L. I., Yan, C., Kimmel, J., Misztal, P. K., Jimenez, J. L., Jayne, J. T., and Worsnop,
- D. R.: Ambient Measurements of Highly Oxidized Gas-Phase Molecules during the
- Southern Oxidant and Aerosol Study (SOAS) 2013, ACS Earth Space Chem., 2, 653–
- 459 672, https://doi.org/10.1021/acsearthspacechem.8b00028, 2018.
- Mohr, C., Thornton, J. A., Heitto, A., Lopez-Hilfiker, F. D., Lutz, A., Riipinen, I., Hong,
- J., Donahue, N. M., Hallquist, M., Petäjä, T., Kulmala, M., and Yli-Juuti, T.: Molecular
- identification of organic vapors driving atmospheric nanoparticle growth, Nat Commun,

- 463 10, 4442, https://doi.org/10.1038/s41467-019-12473-2, 2019.
- Nie, W., Yan, C., Huang, D. D., Wang, Z., Liu, Y., Qiao, X., Guo, Y., Tian, L., Zheng,
- 465 P., Xu, Z., Li, Y., Xu, Z., Qi, X., Sun, P., Wang, J., Zheng, F., Li, X., Yin, R., Dallenbach,
- 466 K. R., Bianchi, F., Petäjä, T., Zhang, Y., Wang, M., Schervish, M., Wang, S., Qiao, L.,
- 467 Wang, Q., Zhou, M., Wang, H., Yu, C., Yao, D., Guo, H., Ye, P., Lee, S., Li, Y. J., Liu,
- 468 Y., Chi, X., Kerminen, V.-M., Ehn, M., Donahue, N. M., Wang, T., Huang, C., Kulmala,
- 469 M., Worsnop, D., Jiang, J., and Ding, A.: Secondary organic aerosol formed by
- 470 condensing anthropogenic vapours over China's megacities, Nat. Geosci., 15, 255–261,
- 471 https://doi.org/10.1038/s41561-022-00922-5, 2022.
- Richters, S., Herrmann, H., and Berndt, T.: Highly Oxidized RO<sub>2</sub> Radicals and
- 473 Consecutive Products from the Ozonolysis of Three Sesquiterpenes, Environ. Sci.
- 474 Technol., 50, 2354–2362, https://doi.org/10.1021/acs.est.5b05321, 2016.
- 475 Song, K., Guo, S., Wang, H., Yu, Y., Wang, H., Tang, R., Xia, S., Gong, Y., Wan, Z., Lv,
- 476 D., Tan, R., Zhu, W., Shen, R., Li, X., Yu, X., Chen, S., Zeng, L., and Huang, X.:
- 477 Measurement report: Online measurement of gas-phase nitrated phenols utilizing a CI-
- 478 LToF-MS: primary sources and secondary formation, Atmos. Chem. Phys., 21, 7917–
- 479 7932, https://doi.org/10.5194/acp-21-7917-2021, 2021.
- Tsiligiannis, E., Hammes, J., Salvador, C., Mentel, T., and Hallquist, M.: Effect of NOx
- on 1,3,5-trimethylbenzene (TMB) oxidation product distribution and particle formation,
- Atmospheric Chemistry and Physics, 19, 15073–15086, https://doi.org/10.5194/ACP-
- 483 19-15073-2019, 2019.
- Wang, Y., Mehra, A., Krechmer, J., Yang, G., Hu, X., Lu, Y., Lambe, A., Canagaratna,
- 485 M., Chen, J., Worsnop, D., Coe, H., and Wang, L.: Oxygenated products formed from
- 486 OH-initiated reactions of trimethylbenzene: autoxidation and accretion, Atmospheric
- Chemistry and Physics, null, null, https://doi.org/10.5194/acp-2020-165, 2020.
- Wang, Z., Ehn, M., Rissanen, M., Garmash, O., Quéléver, L., Xing, L., Monge-Palacios,
- 489 M., Rantala, P., Donahue, N., Berndt, T., and Sarathy, S. M.: Efficient alkane oxidation
- 490 under combustion engine and atmospheric conditions, Communications Chemistry, 4,
- 491 null, https://doi.org/10.1038/s42004-020-00445-3, 2021.
- Wolfe, G. M., Marvin, M. R., Roberts, S. J., Travis, K. R., and Liao, J.: The Framework
- for 0-D Atmospheric Modeling (F0AM) v3.1, Geosci. Model Dev., 9, 3309–3319,
- 494 https://doi.org/10.5194/gmd-9-3309-2016, 2016.
- 495 Yan, C., Nie, W., Äijälä, M., Rissanen, M. P., Canagaratna, M. R., Massoli, P., Junninen,
- 496 H., Jokinen, T., Sarnela, N., Häme, S. A. K., Schobesberger, S., Canonaco, F., Yao, L.,
- Prévôt, A. S. H., Petäjä, T., Kulmala, M., Sipilä, M., Worsnop, D. R., and Ehn, M.:
- 498 Source characterization of highly oxidized multifunctional compounds in a boreal
- 499 forest environment using positive matrix factorization, Atmospheric Chemistry and
- 500 Physics, 16, 12715–12731, https://doi.org/10.5194/acp-16-12715-2016, 2016.

#### Dear Reviewer,

We sincerely thank the reviewer for their time and effort in reviewing our manuscript and for providing valuable comments and constructive suggestions. We appreciate the recognition of our work and the suggestions offered to improve its clarity and scientific rigor. In the responses below, the reviewer's original comments are reproduced in *italic* for clarity. Our point-by-point replies follow each comment and are marked in green. All corresponding changes have been made in the revised manuscript and are marked in blue. Line numbers refer to the revised manuscript unless otherwise noted.

## General comments from reviewer II:

PMF analysis is a widely used receptor model for source apportionment. Running bin-PMF for subranges is an interesting combination to extract more detailed information from the CIMS dataset, where both the sources and sinks can vary greatly. However, the interpretation of the solutions requires great efforts and experience. Although the manuscript is well-structured, several parts of the manuscript need improvement and more detailed clarification. Therefore, I recommend a major revision before the manuscript can be considered for acceptance.

# Specific/technical comments:

Line 145. The assumption that "OOMs detected have the same ionization efficiency as H<sub>2</sub>SO<sub>4</sub>" may not be valid. Previous quantum chemical computations (Hyttinen et al., 2015) have shown that in order to be detected effectively by NO<sub>3</sub>, the highly oxygenated organic molecules need to contain two H-donor functional groups to reach collision-limited detection (typically, at least 7-8 O atoms). However, you "observed OOMs include 3–6 effective oxygen atoms, accounting for 85% of the total signals" (line 206). Can you estimate, at least, the measurement uncertainty introduced by your assumption?

#### **Response:**

We thank the reviewer for this insightful comment. We agree that the assumption of collision-limited detection efficiency comparable to H<sub>2</sub>SO<sub>4</sub> only strictly applies to HOMs, typically with at least 7–8 oxygen atoms and multiple hydrogen donor groups (Hyttinen et al., 2015; Riva et al., 2019). Moderate oxygenated compounds (i.e., with fewer oxygen atoms or lacking strong hydrogen donor groups) may indeed experience lower detection efficiency with the NO<sub>3</sub><sup>-</sup> ion, leading to potential underestimation of their actual ambient concentrations. Riva et al. (2019) illustrated this point by measuring α-pinene ozonolysis products, showing that Nitrate CI-APi-TOF tends to underestimate species with lower oxygen content compared to other ionization methods (Fig. R1). If these monoterpene products are representative of OOMs, Nitrate CI-APi-TOF may significantly underestimate OOMs with lower oxygen numbers, resulting in differences in magnitude compared to other chemical ionization techniques.

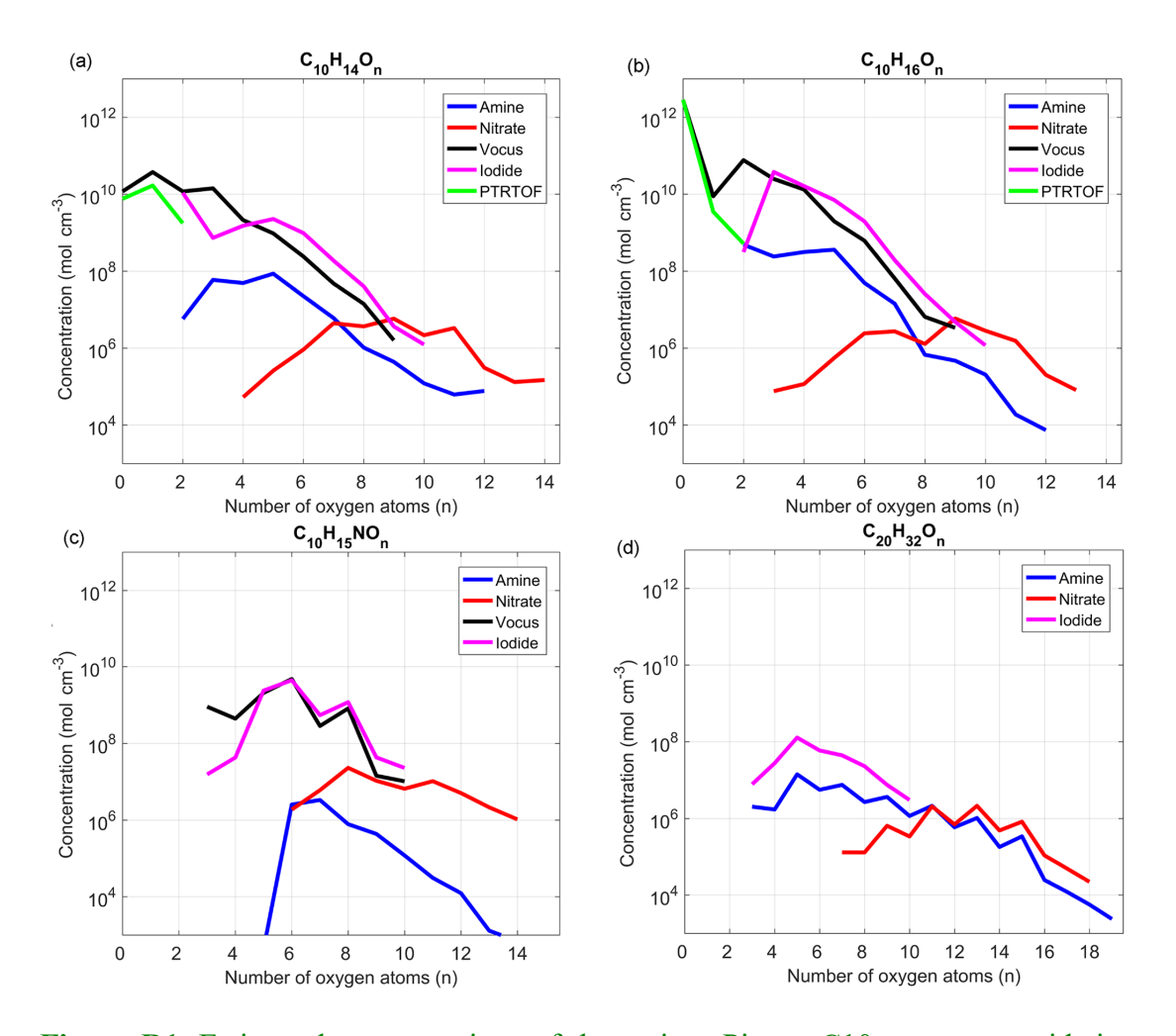


**Figure R1.** Estimated concentrations of the main  $\alpha$ -Pinene C10-monomer oxidation products (a, b), C10-monomer organonitrates (c) and  $\alpha$ -Pinene dimers (d) by the different mass spectrometers deployed in Riva et al. (2019).

540

541

542

543

544545

546

547

548

549

550

551

552

553

554

555

556

557

558

To clarify this point, our earlier mention that 85% of the detected OOM signals fall in the range of 3-6 effective oxygen atoms was based on the functional-group-adjusted oxygen count used for volatility estimation (which does not include nitrate groups). However, when considering the actual number of oxygen atoms in the molecular formulas, the distribution shifts toward higher oxygenation. As shown in the pie chart below (Fig. R2), over half of the total signals are contributed by OOMs with  $n_0 \ge 7$ , which more reasonably satisfies the criteria for efficient NO<sub>3</sub><sup>-</sup> ionization. We acknowledge that the remaining of the detected signals may have a lower ionization efficiency, potentially leading to underestimation of their true concentrations. Given current instrumental limitations, it is difficult to precisely quantify the extent of underestimation across the all OOMs. Still, the assumption of H<sub>2</sub>SO<sub>4</sub>-like ionization efficiency remains the most practical and widely used approach for semi-quantitative analysis in Nitrate CI-APi-TOF studies. Since our work focuses primarily on source apportionment and chemical evolution trends rather than absolute quantification, we believe this assumption is reasonable and does not compromise the central conclusions. This point has been clarified in the revised manuscript.



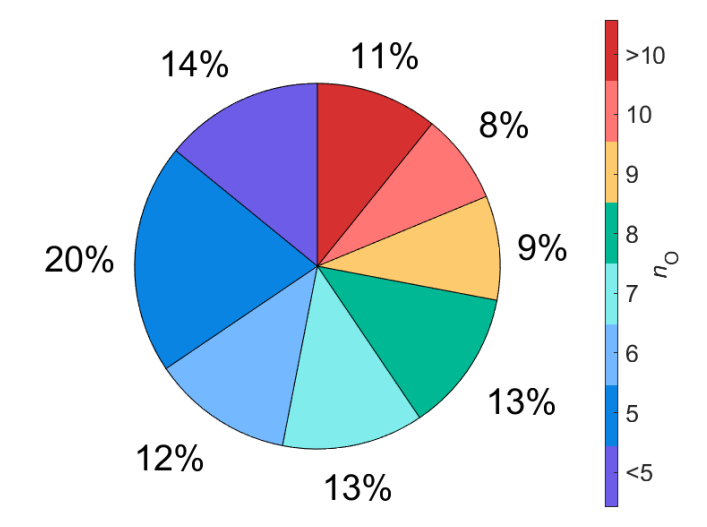


**Figure R2.** Distribution of the number of oxygen atoms  $(n_0)$  for all OOMs identified in this study.

#### Revised text:

*Page 4, Line 145-153:* This assumption is generally valid for highly oxygenated molecules (typically with more than 6 oxygen atoms) due to their efficient clustering with NO<sub>3</sub><sup>-</sup> (Hyttinen et al., 2015; Riva et al., 2019). However, for less oxygenated compounds—particularly those with fewer than six oxygen atoms—ionization efficiency can be substantially lower, resulting in an underestimation of their true concentrations. Although some uncertainty remains in quantifying moderately oxidized species, the assumption remains the most practical and widely used approach for semi-quantitative analysis in related studies.

 Page 4, Section 2.2 instrumentation. Did you use an Eisle NO3 inlet for NO3-CIMS? What was the time resolution of the CIMS dataset used for the PMF analysis? And what are the flow settings for the instruments (e.g., NO3-CIMS, PTR, TOF-ACSM..., maybe summarize the details in a table in the supplementary)? It could also be useful if you could include some of the results/figures on your SA calibration and transmission tests in the supplementary. All these experimental details are important for data quality assessment and inter-study comparisons.

#### **Response:**

We thank the reviewer for pointing out the importance of providing more detailed instrumental information. In this study, the Nitrate-CIMS utilized the Eisele-type NO<sub>3</sub> inlet. The raw data were acquired at a frequency of 1 Hz, and averaged to 30-minute intervals for the PMF analysis. The flow settings for CIMS and other supporting instruments have now been summarized in Table S1 in the Supplementary Information.

Although the ACSM was operated during the campaign, its data were not used in the current analysis. Therefore, we have removed related text from the main manuscript to avoid confusion.

In addition, the calibration results for sulfuric acid and the mass-dependent transmission efficiency test of the APi-TOF have also been included in the Supplement (Fig. S1), as suggested.

#### Revised text:

**Page 5, Line 170-172:** More details about the instruments can be found in the Supplementary Information, including the flow settings of each instrument and the results of the sulfuric acid calibration and transmission efficiency characterization of the CI-APi-TOF (Fig. S1).

# Page 2, Line 30-53 (SI):

S1 Additional details for the instruments

## S1.1 Flow settings of the instruments

For the CI-APi-TOF measurements, ambient air was drawn into a laminar flow reactor through a stainless-steel tube (100 cm long, 3/4 in. diameter) at a flow rate of 10 L/min. A sheath flow of 25 L/min of purified airflow was used to maintain laminar flow conditions within the reactor. Nitrate reagent ions were generated in the sheath flow by exposing air-conditioning nitric acid to a photoionizer X-ray (Model L9491, Hamamatsu, Japan). The PTR-TOF-MS sampled air at a flow rate of 200 mL/min and was connected to an external pump operating at 1.5 L/min to assist in flow control. Flow settings and additional details for other instruments used in this study are summarized in Table S1.

Table S1. Settings for instrumentations used in this study

Measurement	Instruments	Manufacturer	Sample flow	Resolustion
OOMs	CI-APi-TOF	Aerodyne Research, USA/ Tofwerk AG, Switzerland	10 L/min	30 min/1s
VOCs	PTR-TOF	Ion-icon Analytik, Austria	0.2 L/min	10 min/1min
PM <sub>2.5</sub>	SHARP-5030	Thermo Fisher Scientific, USA	16.7 L/min	5 min
$O_3$	TEI-49i	Thermo Fisher Scientific, USA	0.7 L/min	5 min/1 min
$NO_x$	TEI-42i	Thermo Fisher Scientific, USA	1.285 L/min	5 min/1 min
$SO_2$	TEI-43C	Thermo Fisher Scientific, USA	0.5 L/min	5 min/1 min
CO	TEI-48C	Thermo Fisher Scientific, USA	1 L/min	5 min/1 min

S1.2 Sulfuric acid calibration and transmission test

The sulfuric acid calibration factor used in this study was obtained following the method described by Kürten et al. (2012), and the results are shown in Fig. S1. The

transmission efficiency of the CI-APi-TOF as a function of mass was evaluated using perfluorinated organic acids, including Propanoic acid, Pentanoic acid, and Heptanoic acid. The outcome of the transmission test is also presented in Fig. S1.

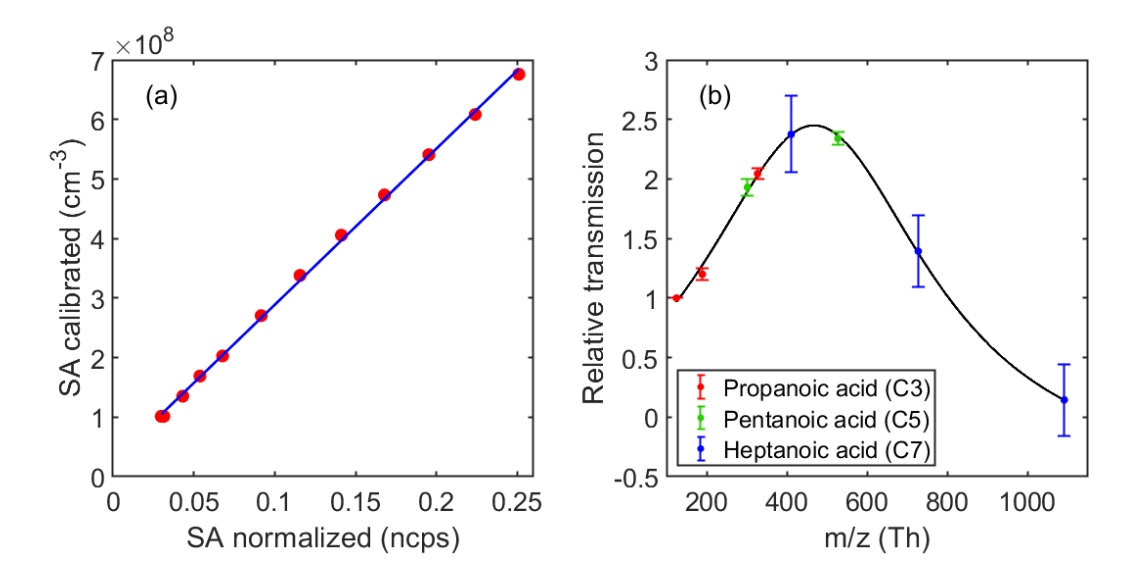


Figure S1. (a) Calibration of sulfuric acid (SA) using the method described by Kürten et al. (2012). (b) Mass-dependent transmission efficiency of the CI-APi-TOF.

Section 3.2.2. For factor D2-AVOC-II, the diurnal variation is bimodal. Why do you think PMF analysis failed to separate this factor into two different factors, one multigenerational oxidation product peaking around 13:00, and one NO<sub>3</sub> oxidation of CHNO compounds peaking around 19:00? Since they have different time variations, PMF should, in principle, be able to distinguish them, right?

## **Response:**

We appreciate the reviewer's thoughtful suggestion. The bimodal diurnal pattern of D2-AVOC-II indeed suggests potential influences from both daytime OH-driven oxidation and nighttime NO<sub>3</sub>-initiated chemistry. One possibility is that this factor represents two distinct sources or processes that were not fully separated by PMF. Alternatively, the bimodal structure may reflect the intrinsic behavior of a single group of compounds influenced by multiple oxidation regimes.

To investigate this, we first examined the evolution of D2-AVOC-II across PMF solutions with increasing numbers of factors (from 8 to 20). As shown in Fig. R3, the mass spectral and temporal characteristics of this factor remain largely consistent throughout the solutions, and no clear separation into two distinct factors occurs, even at high factor numbers. Further increasing the number of factors risks splitting other well-defined factors.

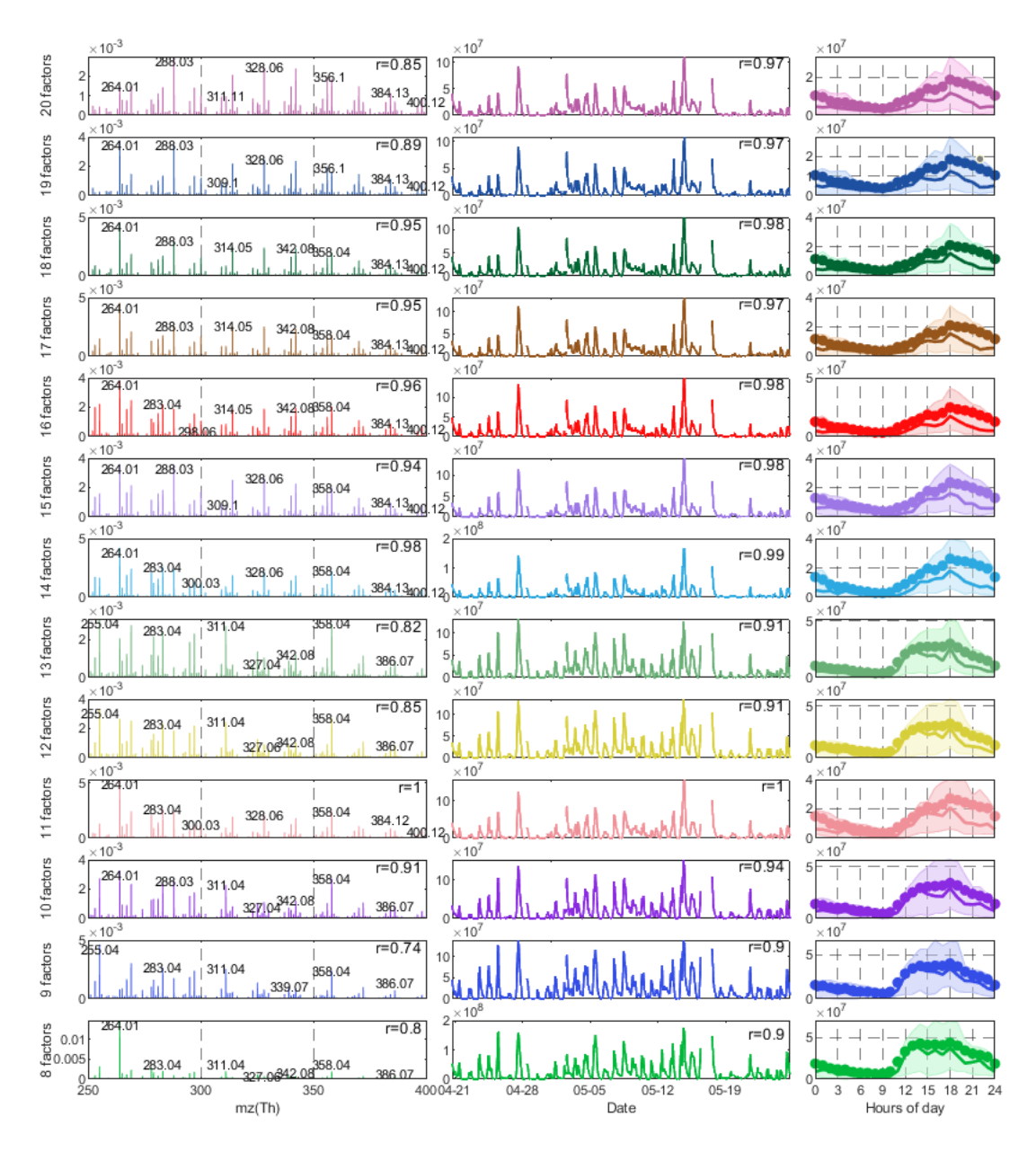


**Figure R3.** Evolution of the D2-AVOC-II factor (in Range 2) across binPMF solutions with 8 to 20 factors. For each solution, the corresponding mass spectrum (left), time series (middle), and diurnal profile (right) are shown. Correlation coefficients (r) represent the similarity of both the mass spectra and time series compared to the corresponding factor in the selected 11-factor solution.

Additionally, we analyzed the diurnal patterns of CHO and CHON species within D2-AVOC-II. As shown in Fig. R4, both classes exhibit bimodal behavior, with significant contributions during both daytime and nighttime. This indicates that the bimodality is not caused by the accidental merging of two unrelated factors, but rather reflects the intrinsic temporal dynamics of the compounds grouped in D2-AVOC-II.

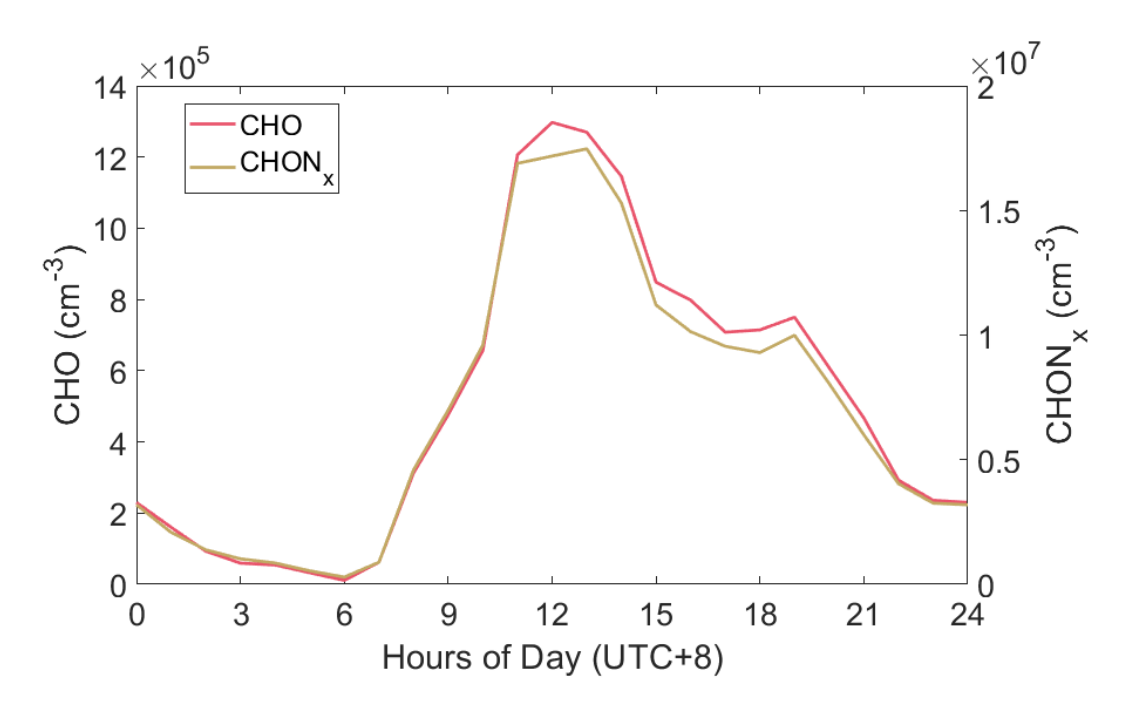


Figure R4. Median diurnal variations of CHO and CHON<sub>x</sub> species of D2-AVOC-II

Taken together, these results suggest that D2-AVOC-II is a coherent factor characterized by contributions from both photochemical and nighttime NO<sub>3</sub> oxidation pathways, rather than an unresolved combination of two separate sources.

Lines 326-327. The statement "higher nighttime values are observed, suggesting some transport influence" is unclear to me. Why does nighttime indicate transport? You've identified a transport factor, so did you find some common compounds? Nighttime concentrations could also result from some sources or compounds with relatively high volatility that linger after daytime formation.

## **Response:**

Thank you for the valuable comment. We agree that our initial suggestion of transport influence based on higher nighttime values may not be fully justified. Upon further reflection, we acknowledge that there is no direct link between nighttime peaks and transport. Although we did identify a transport factor (Trans\_AVOC), and some compounds such as C<sub>x</sub>H<sub>2x-1,2x-3</sub>O<sub>6</sub>N and C<sub>x</sub>H<sub>2x-2</sub>O<sub>8</sub>N<sub>2</sub> are present in both the transport factor and the D4-AVOC-IV factor, these compounds are also observed in other AVOC-related factors, indicating that they are not exclusive to transport.

Upon further analysis, we found that the nighttime enhancements of this factor during certain periods (e.g., P0 in Fig. R5) coincide with elevated  $O_x$  ( $O_3 + NO_2$ ) levels. Since  $O_x$  is less affected by nocturnal NO titration than  $O_3$  alone, it serves as a more robust indicator of photochemically aged air and regional background influence. This covariation suggests that some of the nighttime enhancements may be associated with

transport influence. But given the factor's distinct diurnal pattern with clear daytime peaks and lack of clear transport signatures, we consider transport influence to be minor and have removed this speculation in the revised text to avoid potential misinterpretation.

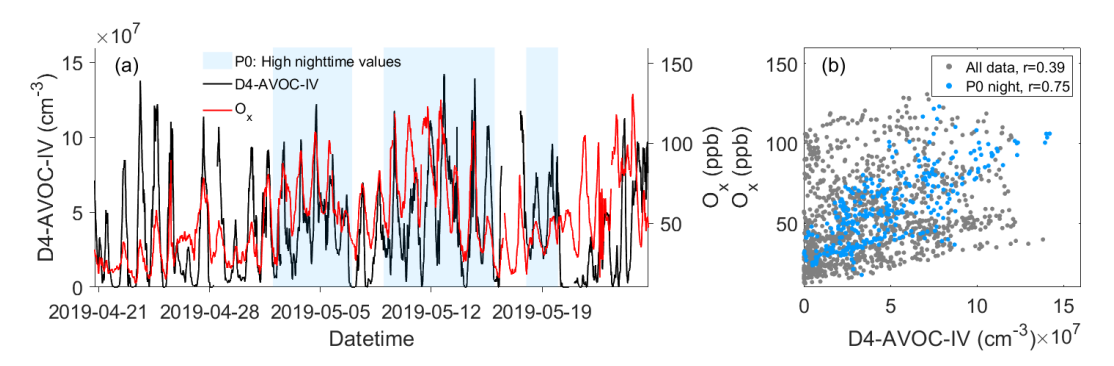


**Figure R5.** (a) Time series of the D4-AVOC-IV factor (black) and  $O_x$  (red) with blue shaded areas representing periods of high nighttime values (P0) identified for further analysis. (b) Correlation between D4-AVOC-IV and  $O_x$ , with blue points representing nighttime data (18:00-6:00 LT) during the P0 period.

Line 345. Could these C10 compounds be partly formed through C5-RO2 + C5-RO2 rather than from monoterpene, because they are grouped in this Isoprene-related factor by PMF? Similarly, for section 3.3.4, factor N4-SQT, could there be C15 compounds formed from C5-RO2 + C10-RO2 dimer?

## **Response:**

We greatly appreciate this insightful suggestion. The potential formation of  $C_{10}$  and  $C_{15}$  compounds through dimerization of different RO<sub>2</sub> radicals (e.g.,  $C_5$ -RO<sub>2</sub> +  $C_5$ -RO<sub>2</sub> or  $C_5$ -RO<sub>2</sub> +  $C_{10}$ -RO<sub>2</sub>) is indeed a plausible pathway, particularly under nighttime conditions at our site, where we observed substantial concentrations of both  $C_5H_8NO_5$  and  $C_{10}H_{16}NO_x$  RO<sub>2</sub> radicals. However, for the D5-IP factor, which is primarily a daytime factor, RO<sub>2</sub> radicals are expected to terminate predominantly via reaction with NO rather than through bimolecular RO<sub>2</sub>–RO<sub>2</sub> reactions. This makes significant dimerization within this factor less likely, although we cannot completely exclude the possibility.

In contrast, the N4-SQT factor is a nighttime factor, and thus RO<sub>2</sub>–RO<sub>2</sub> reactions could plausibly contribute to the formation of certain C15 species. Nevertheless, we also observe C<sub>15</sub>H<sub>24</sub>NO<sub>x</sub> compounds that can be attributed to the oxidation of sesquiterpene precursors. Therefore, while we cannot rule out the contribution from dimerization (e.g., C5-RO<sub>2</sub> + C10-RO<sub>2</sub>), the presence of sesquiterpene-derived RO<sub>2</sub> supports the interpretation that these C15 products are at least partly derived from SQT oxidation.

We have revised the manuscript accordingly to incorporate this discussion and to reflect the mechanistic uncertainty.

709 Revised text:

- Page 13, Line 438-440: Due to the relatively high NO concentration during the daytime at this site, it is unlikely that these C<sub>10</sub> substances originate from C<sub>5</sub> RO<sub>2</sub>+C<sub>5</sub>
- 712 RO<sub>2</sub>.
- 713 *Page 15, Line 511-517:* However, some of the C<sub>15</sub>H<sub>24</sub>O<sub>x</sub>N<sub>2</sub> species, particularly
- 714 those with higher oxygen content, are likely products of C<sub>5</sub>-RO<sub>2</sub> and C<sub>10</sub>-RO<sub>2</sub>
- 715 dimerization reactions, given the presence of C<sub>5</sub>H<sub>8</sub>NO<sub>5</sub> and C<sub>10</sub>H<sub>16</sub>O<sub>x</sub>N radicals
- observed in other nighttime factors and their similar diurnal patterns. However, due to
- 717 the detection of C<sub>15</sub> RO<sub>2</sub>, these C<sub>15</sub> substances are more likely to originate from
- 718 sesquiterpene precursors.

719

- 720 Lines 360-361. A repeated sentence, "This RO2 360 radical originates from NO3-
- 721 initiated oxidation of isoprene."

## 722 **Response:**

- We thank the reviewer for pointing this out. The redundant sentence has been
- 724 removed in the revised manuscript.

725

730

- Figure 2. It would be helpful for readers if you could label each factor with the
- 727 molecular formulae of their highest peaks for quick visual reference (e.g., a quick
- 728 glance at the C numbers). Also, a pie chart showing the contribution of each factor to
- 729 the total signal intensity could be informative.

## **Response:**

- We thank the reviewer for the helpful suggestion. As recommended, we have revised
- Figure 2 to include molecular formula labels for the highest peaks of each factor,
- 733 allowing for a quick visual reference to their dominant carbon numbers and chemical
- 734 compositions. In addition, a pie chart summarizing the contribution of each factor to
- 735 the total signal intensity has been added to the Supplementary Information (Fig. S6).
- 736 These additions enhance the clarity of the figure and provide a more intuitive overview
- of the chemical composition and relative importance of each factor.

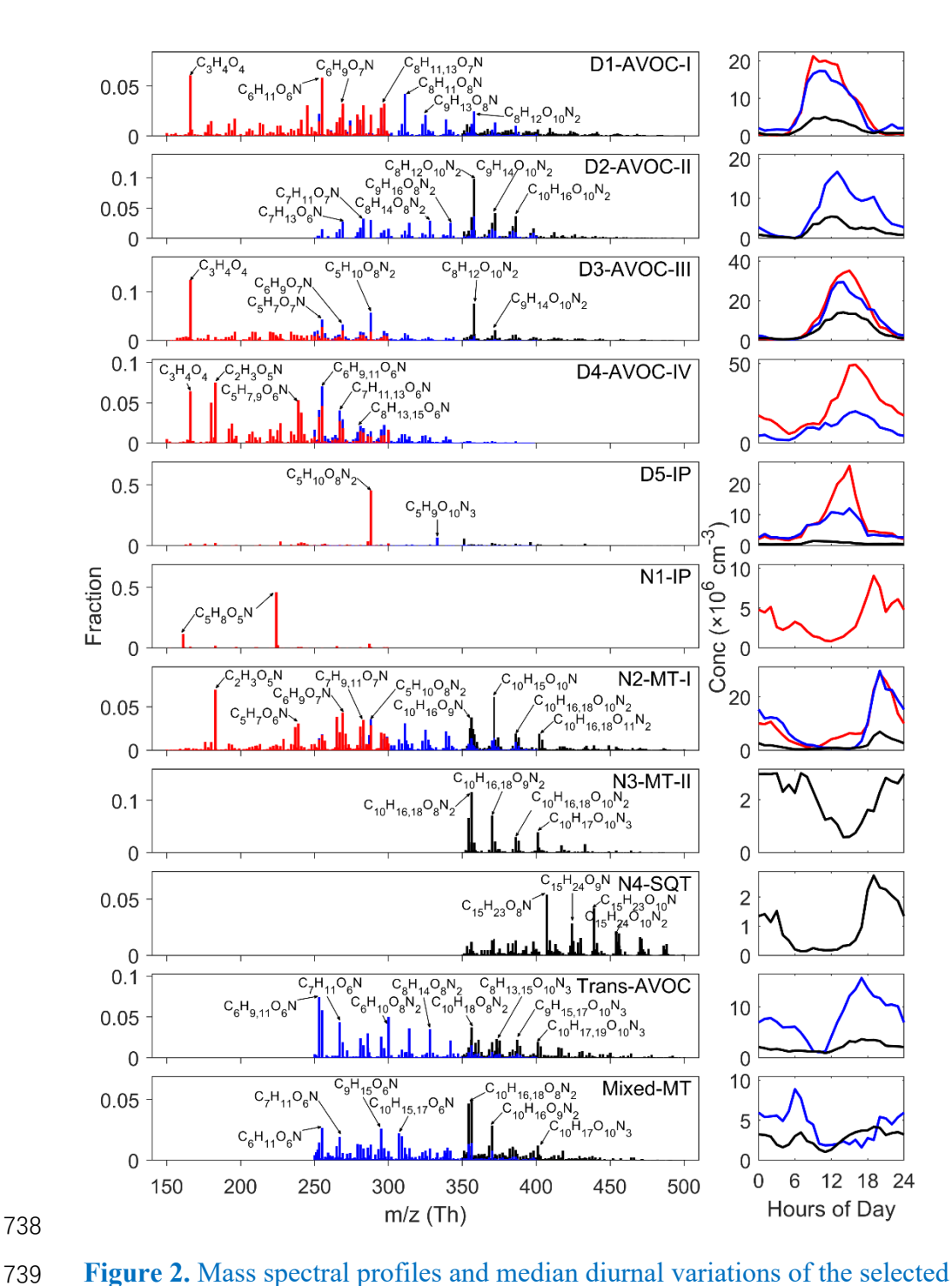
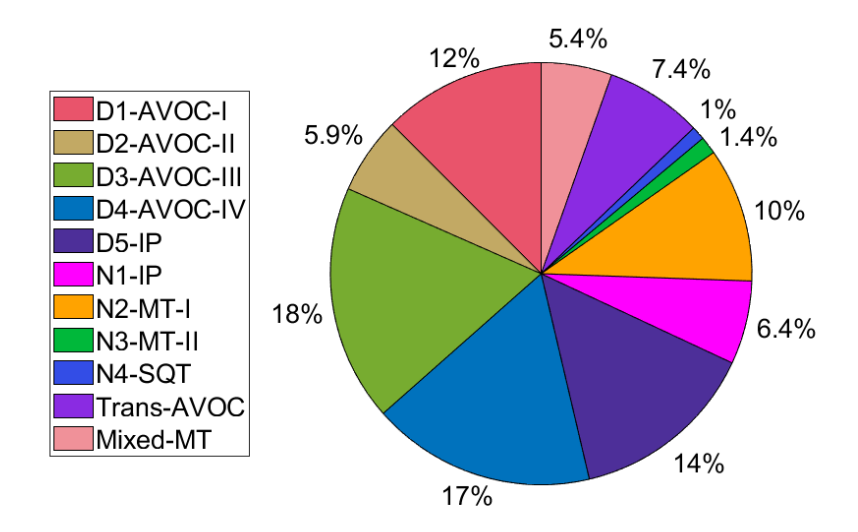


Figure 2. Mass spectral profiles and median diurnal variations of the selected binPMF factors, and the elemental formulas of major peaks are labeled above them. Factors describing the similar process were assembled, red for Range 1, blue for Range 2 and black for Range 3.

740

741

742



**Figure S6.** Relative contributions of the 11 factors to the total concentration of measured OOMs.

Lines 396-397. Can you provide plots for the diurnal variation of dinitrates  $C_{10}H_{16,18}O_{8-13}N_2$  and trinitrates  $C_{10}H_{17}O_{10-13}N_3$ ? The diurnal plot of this factor will be the average of all organic nitrate, while the dinitrates ( $NO_3$ - $RO_2$  + NO or monoterpenes contain two C=C bonds that reacted twice with  $NO_3$ ?) and trinitrates (further oxidation of dinitrates?) should only appear in the early morning, based on your hypothesis, right?

### **Response:**

Thank you for the constructive comment. We have now added the diurnal variation plots of dinitrates (C<sub>10</sub>H<sub>16,18</sub>O<sub>8-13</sub>N<sub>2</sub>) and trinitrates (C<sub>10</sub>H<sub>17</sub>O<sub>10-13</sub>N<sub>3</sub>) as Fig. R6. Contrary to the hypothesis that these species should appear only in the early morning, our results show that both dinitrates and trinitrates exhibit broader temporal distributions.

It is also important to note that these C10 compounds are not exclusive to the N3-MT-II factor; other factors contribute to them to varying degrees. Therefore, their diurnal variations reflect a combination of sources and cannot be taken as representative of the N3-MT-II factor alone. In contrast, the PMF analysis groups species based on their co-variation across time, and the N3-MT-II factor as a whole shows a consistent nighttime-to-early-morning profile. We hypothesize that these compounds could be secondary oxidation products from nocturnal processes, such as the initial oxidation by NO<sub>3</sub> radicals, followed by further OH radical-driven oxidation in the morning. Similarly, some of the nighttime concentrations might be the result of daytime oxidation products that undergo additional NO<sub>3</sub>-initiated oxidation during the night. Overall, the N3-MT-II factor represents a multi-generational oxidation product, involving multiple

oxidants during the transition between day and night. For clarity, I have revised the relevant paragraph in the original text.

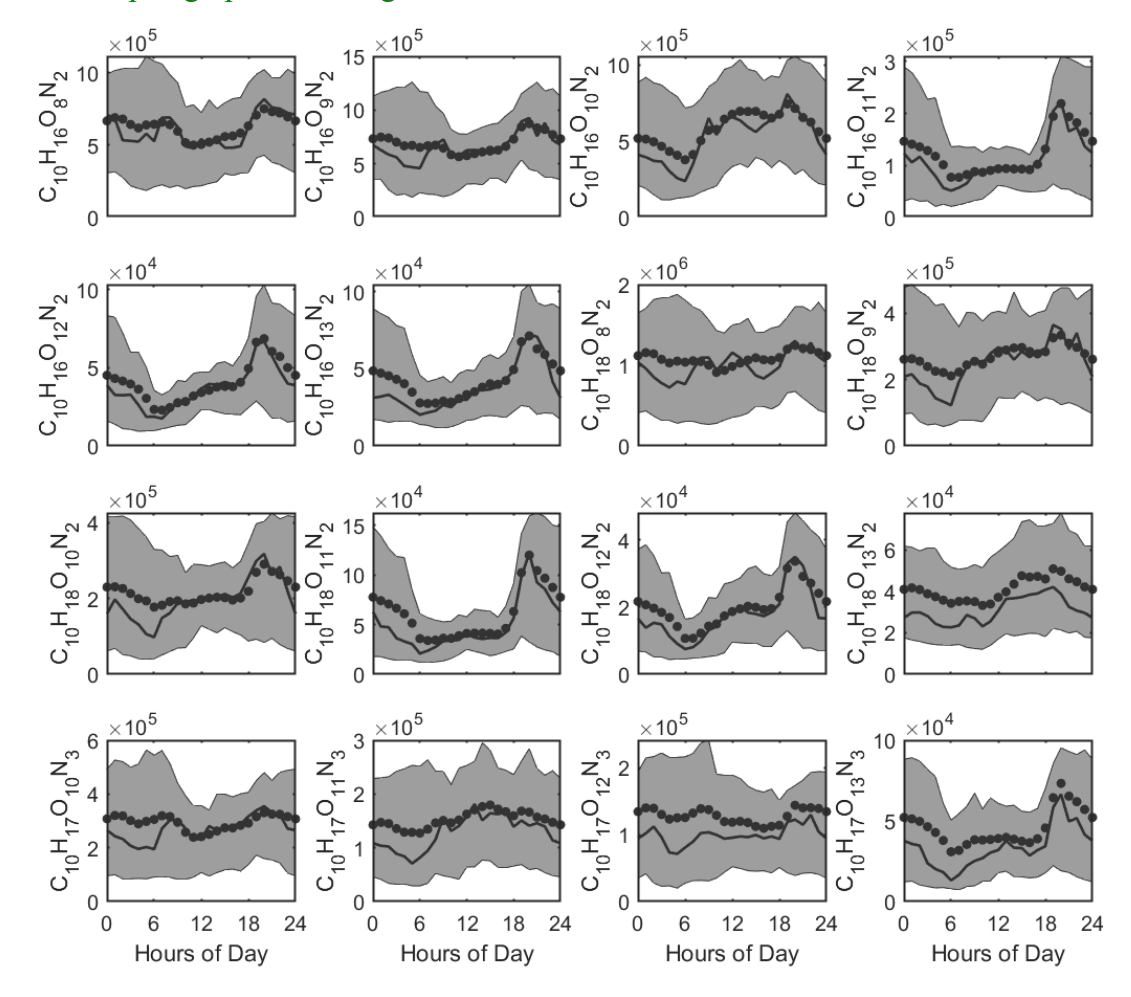


**Figure R6.** Diurnal variations of C10 dinitrates and trinitrates. Each subplot represents the hourly variation of a specific compound, with the shaded region indicating the interquartile range (between upper and lower quartiles), the solid line representing the median, and the scattered points indicating the mean values.

#### Revised text:

*Page 14, Line 493-503:* This suggests that NO<sub>3</sub>-initiated oxidation of monoterpenes at night is followed by further oxidation in the morning, potentially involving OH and O<sub>3</sub>, leading to the observed multi-nitrate species. Furthermore, some of the nighttime concentrations may arise from daytime oxidation products that undergo additional NO<sub>3</sub>-driven oxidation during the night. Overall, this factor represents multi-generational oxidation products, involving various oxidants during the transition between day and night.

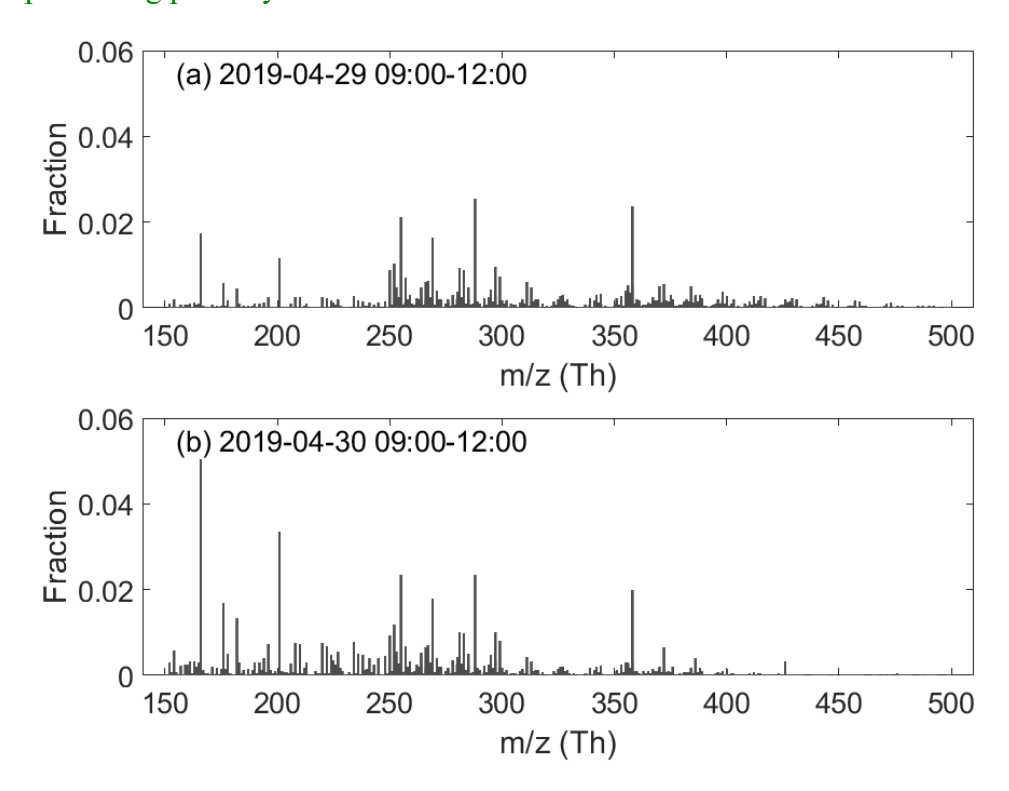
Lines 464-467. I don't understand why the sub-range PMF "reveals how chemical conditions and processing pathways evolve over time, reflected by temporal variations in the relative contributions of spectral sub-ranges to individual factors". Like

traditional PMF, your sub-range PMF should also generate static mass spectra for each factor, right? Then, how were you able to obtain mass spectra for factors D3-AVOC-III and D1-AVOC-I under different conditions? Please explain this in your method part as well.

### **Response:**

You are correct that traditional PMF generates static mass spectra for each factor. In our approach, we used a subrange PMF that allows for the identification of factors across different spectral subranges. Each factor is derived from a combination of subranges that exhibit similar temporal variation, grouped together as the same factor. However, due to differences in volatility and chemical composition across subranges, the temporal evolution of the same factor will not be perfectly consistent across all subranges. This can be seen in the correlation coefficients in Fig. 3, where some factors show lower than perfect correlations (r<1) across subranges.

As a result, the relative contribution of each subrange to a factor will evolve over time. For factors with contributions from multiple subranges, the mass spectra will vary with time, reflecting these dynamic shifts in the subrange contributions. The more subranges we include, the finer the temporal variation we can analyze, and this may reveal more detailed information about the underlying chemical processes. For example, we provide an analysis of D3-AVOC-III in Fig. R7, showing its average mass spectra for different time periods. The proportion of R1 in (a) is lower than in (b), while the proportion of R3 in (a) is higher than in (b). Our subsequent analysis builds on this dynamic temporal variation to explore the underlying chemical conditions and processing pathways.



- Figure R7. Average mass spectra of the D3-AVOC-III factor during different time periods: (a) 09:00–12:00 on April 29, 2019, and (b) 09:00–12:00 on April 30, 2019.
- We will expand on this explanation in the methods section of the revised manuscript to provide more clarity.

## 816 Revised text:

- *Page 6, Line 195-202:* The relative changes in the source factor profiles between the different sub-ranges contribute to the dynamic nature of the combined factor spectra. Specifically, variations in the mass spectral features across the sub-ranges lead to distinct temporal and compositional changes in the final factor profiles. This dynamic analysis approach enables better resolution of source processes and provides a more robust representation of the underlying sources. By minimizing sink-induced variations and leveraging the temporal and compositional overlap between the ranges, we achieve improved factor separation and identification.
- Page 18, Line 610-617: Specifically, as different sub-ranges are combined, the relative intensities of these ranges fluctuate, demonstrating how variations in chemical reactivity and environmental conditions influence the composition and formation of OOMs. These dynamic observations better represent atmospheric processes, where constantly changing oxidation conditions alter OOM distributions across different volatility ranges. The ability to track these variations in real time allows for a more nuanced understanding of how source and sink processes interact under different atmospheric conditions.

Figures 6 and S6 (and also Figures 7 and S7), what is the unit for "difference of profiles"? Using relative difference (e.g., normalized to "Low T/NOx" or "Low CS") might make the comparison clearer and easier to understand.

# **Response:**

Thank you for your valuable suggestion. We agree that using relative changes would make the comparison clearer and easier to understand. We attempted to replot the figure using the relative difference, and the results indeed lead to the same conclusions. However, the new plot (Fig. R8) is not as visually appealing, as most of the peaks are clustered around similar values. Upon analyzing this result, we found an explanation. The relative difference after normalization is a ratio form (H-L)/L=H/L-1, and for single-range PMF factors, the spectra for any two time periods are identical. Therefore, the ratio of the peak values between any two time periods is constant. As a result, parts of the plot corresponding to mass ranges with only one PMF analysis (150-250 Th, 300-350 Th, and 400-500 Th) show a constant value. Some peaks deviate from this constant value because concentrations below the detection limit were excluded for certain peaks. Ultimately, we decided to retain the original plotting method.

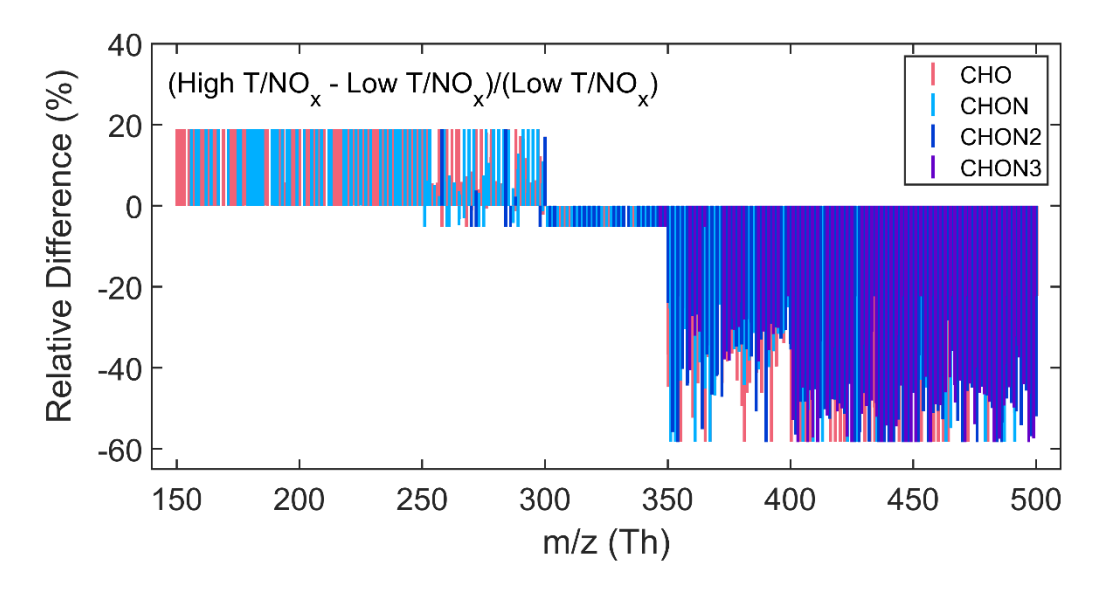


**Figure R8.** Relative difference between the average mass spectra of D3-AVOC-III under high  $T/NO_x$  (above the upper quartile) and low  $T/NO_x$  (below the lower quartile) conditions, normalized to low  $T/NO_x$ .

Line 497. What exactly is the "T/NOx ratio"? They have different units, so, the meaning of this ratio is unclear. What does a high or low value indicate chemically or physically? Why not directly use T or NOx, or make one plot vs T but colored by NOx, for example?

# Response:

Originally, our intention was to separately investigate the effect of temperature on nitrogen-containing OOMs. As shown in Fig. R9, the trends observed using temperature alone are largely consistent with our main conclusions. However, analyzing temperature in isolation is not entirely comprehensive, since NO<sub>x</sub> levels also play a crucial role in determining the nitrogen content of oxidation products. To better isolate the temperature effect under comparable NO<sub>x</sub> levels, we adopted a ratio-based approach (T/NO<sub>x</sub>). While not dimensionally rigorous, this metric conceptually represents the influence of temperature under a fixed NO<sub>x</sub> condition—essentially, "how temperature modulates nitrogen incorporation into OOMs when NO<sub>x</sub> availability is constrained." This simplification allowed us to group the data more clearly by combined chemical conditions, facilitating interpretation. That said, we agree this representation may be confusing, and we have added clarification in the revised text.

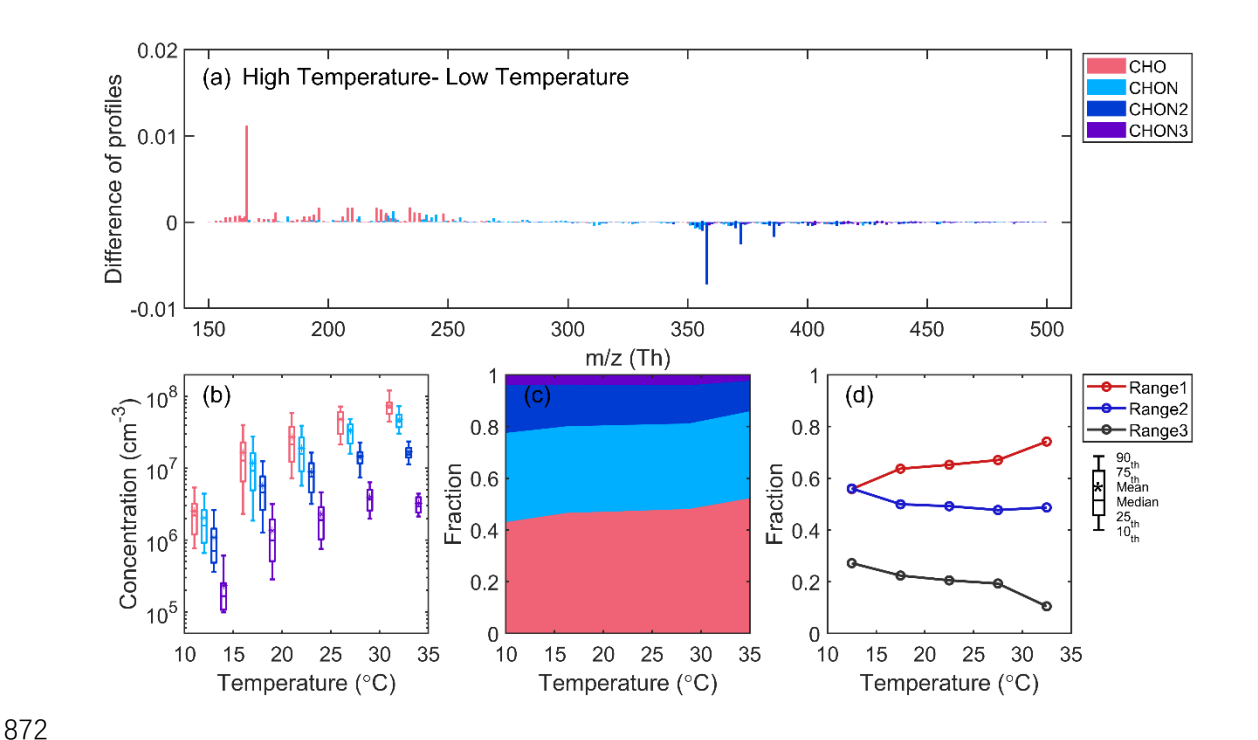


**Figure R9.** Characteristics of D3-AVOC-III under varying temperature conditions. (a) Difference between the average mass spectra of D3-AVOC-III under high temperature (above the upper quartile) and low temperature (below the lower quartile) conditions. (b) Boxplots of the concentrations of CHO and CHON<sub>x</sub> (x = [1,3]) species binned by temperature in each 5 °C interval. (c) Fractional contributions of CHO and CHON<sub>x</sub> (x = [1,3]) species for different temperature conditions. (d) Evolution of fractional contributions of three sub-ranges as a function of temperature.

## Revised text:

*Page 19, Line 642-652:* While temperature and NO<sub>x</sub> individually influence oxidation chemistry, analyzing them in isolation may obscure their combined effects—especially since NO<sub>x</sub> levels tend to decrease with increasing temperature due to enhanced photochemical activity and atmospheric mixing. To better isolate the influence of temperature under comparable NO<sub>x</sub> conditions, we adopted the ratio of temperature to NO<sub>x</sub> (T/NO<sub>x</sub>) as a simplified metric. Although this ratio does not represent a physically defined parameter, it serves as a practical index allowing for clearer grouping of data and a more interpretable assessment of compositional differences.

Lines 510-512. Do you have references to support this argument that "elevated temperatures favor the  $RO + NO_2$  channel, reducing the formation of  $RONO_2$  from the  $RO_2 + NO$  reaction"? Should the product of  $RO+NO_2$  also be thermally unstable? Why does higher T favor  $RO + NO_2$  than  $RO_2 + NO$ ?

## **Response:**

Thank you for pointing this out. We are sorry for the confusion caused by our wording — the term " $RO + NO_2$  channel" was a misstatement. Here, our discussion refers specifically to the reaction between  $RO_2$  and NO, which primarily proceeds via two branches:

$$RO_2 + NO \rightarrow RO + NO_2$$
 R1a

900 
$$RO_2 + NO \rightarrow RONO_2$$
  $R1b$ 

Experimental studies have shown that the branching ratio of the RONO<sub>2</sub> formation pathway (R1b) decreases with increasing temperature, meaning that elevated temperatures favor the RO + NO<sub>2</sub> pathway (R1a) over the RONO<sub>2</sub> formation (R1b). This temperature dependence has been quantified in several studies (Cassanelli et al., 2007; Butkovskaya et al., 2010; Perring et al., 2013). The observed decline in nitrogencontaining compound fractions under higher temperature conditions in our data is consistent with this known chemical behavior. We will revise the original sentence for clarity and include the appropriate references in the manuscript.

#### Revised text:

*Page 20, Line 663-668:* This trend reflects shifts in RO<sub>2</sub> radical chemistry. Under high NO<sub>x</sub> conditions, RO<sub>2</sub> primarily reacts with NO, and this reaction has two main pathways: formation of RO + NO<sub>2</sub> or organic nitrates (RONO<sub>2</sub>). Previous studies have shown that increasing temperature suppresses the nitrate-forming branch in favor of the RO + NO<sub>2</sub> branch, thus reducing the formation of RONO<sub>2</sub> (Cassanelli et al., 2007; Butkovskaya et al., 2010; Perring et al., 2013).

Line 554. What is the typical range of CS observed at your site? Is 0.05 s<sup>-1</sup> considered extremely high in your context?

## **Response:**

The CS values observed during the campaign ranged from 0 to 0.05 s<sup>-1</sup>, with 0.05 s<sup>-1</sup> being at the upper end of the distribution. To clarify this point, we have added the corresponding time series and diurnal pattern of CS (Fig. R10).

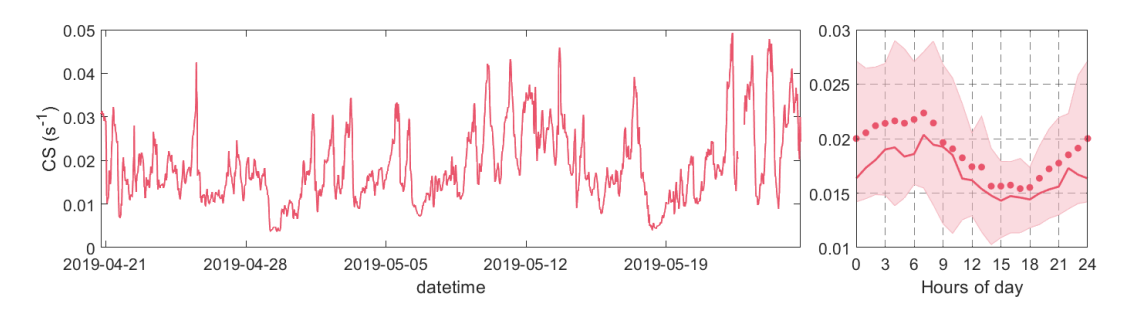


**Figure R10.** Time series and diurnal variation of the condensation sink (CS) during the campaign.

Lines 558-559. The sentence "condensation processes under high CS conditions act as a controlling mechanism for species partitioning" is very confusing? Should volatility and OA mass always control the gas-particle partitioning? And CS means condensation sink, of course under higher CS one would expect higher rate of condensation? Please clarify.

## **Response:**

Thank you for pointing out the ambiguity. The original sentence was indeed unclear and may have been misleading. Our intention was not to refer to gas-particle partitioning, which is governed primarily by volatility and OA mass, but rather to describe the relative abundance of gas-phase OOMs with different volatilities as a function of the condensation sink (CS).

Specifically, at low CS levels, the increase in OOM signals is primarily driven by enhanced chemical formation, and species across a wide volatility range show simultaneous increases. However, at high CS levels, condensation loss starts to dominate over chemical production, particularly for low-volatility OOMs. As a result, the relative contribution of lower-volatility compounds begins to decline, whereas semi-volatile compounds remain more abundant in the gas phase.

We will revise the original sentence accordingly to improve clarity and remove the confusion around partitioning processes.

## Revised text:

*Page 22, Line 729-732:* This observation aligns with prior theoretical predictions and laboratory findings (Peräkylä et al., 2020), which suggest that under high CS conditions, condensation dominates over chemical formation in shaping the gas-phase abundance of different volatility classes of OOMs.

Figures 6d and 7d. What does this fractional contribution analysis mean? Because at each CS bin, the sum of R1, R2, and R3 seems to be larger than 1, which is confusing. Also, your explanation in lines 561-564 is misleading. With the increases in CS, all mass ranges should decrease because of enhanced condensation, right? It is because R3 and R2 condensed more than R1, making the relative fraction of R1 increase. Therefore, I think absolute concentrations would be more informative than fraction contributions here.

### **Response:**

We appreciate the reviewer's constructive comments and the opportunity to clarify. The "fractional contribution" in Figs. 6d and 7d refers to the relative contribution of each spectral sub-range to the total signal within the entire analyzed mass range (150–500 Th). Due to the intentional 50 Th overlaps between adjacent sub-ranges (e.g., 250–300 Th and 350–400 Th), the summed concentrations of all sub-ranges exceed the total,

resulting in fractional contributions summing to values greater than 1. We have now added a clarification on this point.

In response to the reviewer's suggestion, we also generated alternative plots showing the absolute concentrations of R1–R3 as functions of temperature/NO<sub>x</sub> and condensation sink (Fig. S12). These results confirm our previous interpretation: all subranges of D1-AVOC-I increase with CS initially, consistent with pollution-driven chemical production. However, under very high CS conditions, R2 and R3 begin to decline, while R1 continues to increase, indicating a volatility-dependent loss from the gas phase due to condensation. Thus, both the fractional contribution and absolute concentration perspectives are complementary and valuable. We agree that the original explanation may have been misleading and have revised the relevant text to more accurately reflect the interplay between production and condensation.

#### Revised text:

Page 22, Line 733-741: We analyzed the fractional contributions of different subranges under varying CS conditions. Due to their lower volatility, higher m/z species in R2 and R3 are more susceptible to loss through condensation under high CS, while lower m/z species in R1 (likely SVOCs and LVOCs) are less affected. As a result, the relative contribution of R1 increases with CS, whereas those of R2 and R3 gradually decrease. This trend highlights a volatility-dependent partitioning effect, where enhanced condensation preferentially removes less-volatile compounds from the gas phase under elevated CS conditions, as also reflected by the absolute concentration changes of sub-ranges under increasing CS (Fig. S12).

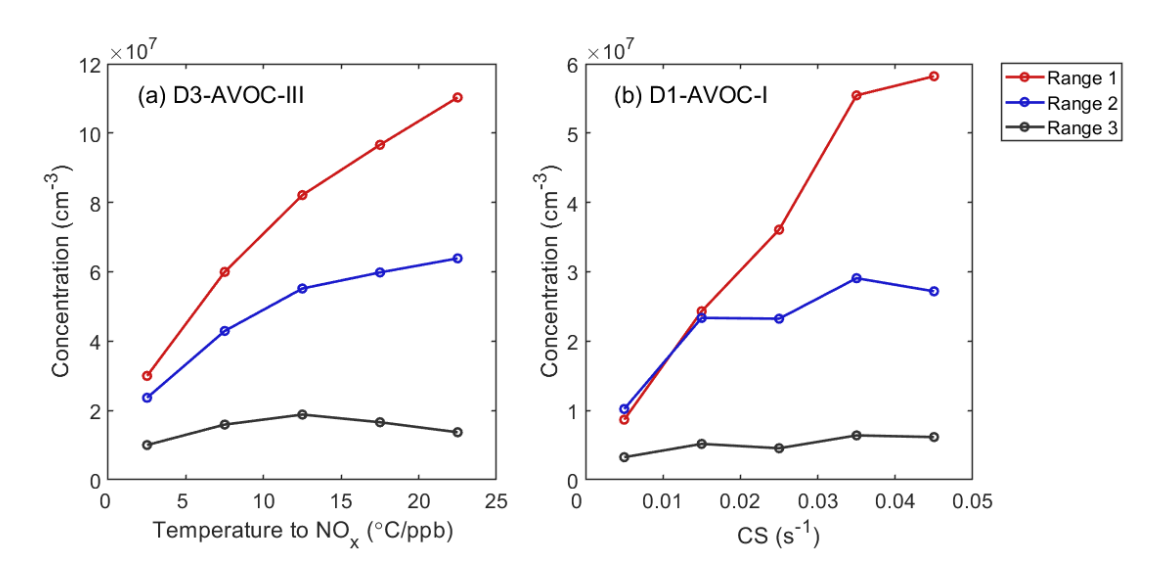


**Figure S12.** Evolution of concentrations of three sub-ranges of (a) D3-AVOC-III with T/NO<sub>x</sub> ratio, and (b) D1-AVOC-I with CS.

## 992 **Reference:**

- 993 Butkovskaya, N., Kukui, A., and Le Bras, G.: Pressure and Temperature Dependence
- of Ethyl Nitrate Formation in the C<sub>2</sub> H<sub>5</sub> O<sub>2</sub> + NO Reaction, J. Phys. Chem. A, 114, 956–
- 995 964, https://doi.org/10.1021/jp910003a, 2010.
- 996 Cassanelli, P., Fox, D. J., and Cox, R. A.: Temperature dependence of pentyl nitrate
- 997 formation from the reaction of pentyl peroxy radicals with NO, Phys. Chem. Chem.
- 998 Phys., 9, 4332, https://doi.org/10.1039/b700285h, 2007.
- 999 Hyttinen, N., Kupiainen-Määttä, O., Rissanen, M. P., Muuronen, M., Ehn, M., and
- 1000 Kurtén, T.: Modeling the Charging of Highly Oxidized Cyclohexene Ozonolysis
- 1001 Products Using Nitrate-Based Chemical Ionization, J. Phys. Chem. A, 119, 6339–6345,
- 1002 https://doi.org/10.1021/acs.jpca.5b01818, 2015.
- Kürten, A., Rondo, L., Ehrhart, S., and Curtius, J.: Calibration of a Chemical Ionization
- Mass Spectrometer for the Measurement of Gaseous Sulfuric Acid, J. Phys. Chem. A,
- 1005 116, 6375–6386, https://doi.org/10.1021/jp212123n, 2012.
- 1006 Peräkylä, O., Riva, M., Heikkinen, L., Quéléver, L., Roldin, P., and Ehn, M.:
- Experimental investigation into the volatilities of highly oxygenated organic molecules
- 1008 (HOMs), Atmos. Chem. Phys., 20, 649–669, https://doi.org/10.5194/acp-20-649-2020,
- 1009 2020.
- 1010 Perring, A. E., Pusede, S. E., and Cohen, R. C.: An Observational Perspective on the
- 1011 Atmospheric Impacts of Alkyl and Multifunctional Nitrates on Ozone and Secondary
- 1012 Organic Aerosol, Chem. Rev., 113, 5848–5870, https://doi.org/10.1021/cr300520x,
- 1013 2013.
- Riva, M., Rantala, P., Krechmer, J. E., Peräkylä, O., Zhang, Y., Heikkinen, L., Garmash,
- 1015 O., Yan, C., Kulmala, M., Worsnop, D., and Ehn, M.: Evaluating the performance of
- 1016 five different chemical ionization techniques for detecting gaseous oxygenated organic
- 1017 species, Atmos. Meas. Tech., 12, 2403-2421, https://doi.org/10.5194/amt-12-2403-
- 1018 2019, 2019.

1019

1020

1021